Département de géographie et télédétection
Faculté des lettres et sciences humaines
Université de Sherbrooke

Textural Analysis for Urban Class Discrimination Using IKONOS Imagery

---

L'analyse texturale pour la discrimination des classes urbaines sur des images IKONOS

SHAHID KABIR

A thesis presented in partial fulfilment of the requirements for the degree of Master of Science in Geography, specialization in Geomatics

Fall 2003

Director of Research: Dr. Dong-Chen He

Co-Director of Research: Dr. Goze Bertin Bénié

Jury Members:

Dr. Dong-Chen He (Département de géographie et télédétection, Université de Sherbrooke)

Dr. Goze Bertin Bénié (Département de géographie et télédétection, Université de Sherbrooke)

Dr. Wei Li (Centre de recherche sur les communications, Ottawa)

Textural Analysis for Urban Class Discrimination Using IKONOS Imagery

Abstract

High spatial resolution imagery can be a very significant source of detailed land cover and land use data necessary for better urban planning and management, which is becoming increasingly important due to the growing human population. However, traditional methods, based on spectral data, used to extract this information from remote sensing imagery have proven to be unsuitable for high-resolution images. Spatial data, or texture, has been widely investigated as a supplement to spectral data for the analysis of complex urban scenes. However, the application of these techniques on high spatial resolution imagery, such as those obtained by the IKONOS satellites, has yet to be studied. This research, therefore, focuses on the extraction of texture features through the use of the Grey Level Co-occurrence Matrix texture analysis technique, which are then combined with the spectral data in the Maximum Likelihood Classification approach, as a method for obtaining more accurate urban land cover and land use information from high spatial resolution IKONOS imagery.

In this study, classifications were done using three datasets: a spatial dataset consisting of three texture channels (Mean, Homogeneity and Dissimilarity), a spectral dataset consisting of four spectral channels (Red, Green, Blue and N-IR), and a combination dataset (spatial and spectral). The results show that the spatial dataset produced an overall classification accuracy of 73.5 %. The spectral dataset produced a slightly higher overall classification accuracy of 78.9 %, an increase over the spatial dataset of 5.4 %. The combination dataset produced the highest overall classification accuracy of 86.1 %, which is an increase of 7.2 % over the spectral dataset. These results demonstrate great potential for the contribution of texture and high-resolution images in deriving more accurate and detailed urban information.

L'analyse texturale pour la discrimination des classes urbaines sur des images IKONOS

Sommaire

À mesure que la demande augmente pour une meilleure gestion d'utilisation du sol, à cause de la croissance continuelle de la population humaine, les images de haute résolution s'avèrent très utiles à fournir des données urbaines plus détaillées de couverture du sol et d'utilisation du sol des milieux urbains. Cependant, les organismes publics et privés ont besoin d'outils efficaces pour l'exploitation de ces images.

Les méthodes traditionnelles de classification pour analyser et cartographier le milieu urbain présentent quelques obstacles principaux. Les terrains sont composés de matériaux naturels et artificiels ayant des propriétés spectrales presque identiques pouvant présenter une grande confusion entre les classes. Cette confusion peut également être provoquée par le fait que les pixels qui représentent le même type de couverture du sol n'auront pas nécessairement la même information spectrale due au bruit dans les données, aux effets atmosphériques et à la variation naturelle dans le type de couverture du sol (Smith and Fuller, 2001). D'autre part, les résolutions spatiales de la plupart des données satellitaires précédentes sont trop basses pour permettre la discrimination efficace des objets urbains, ce qui rend ainsi le processus de classification bien plus difficile (Kiema, 2002). Un autre désavantage de ces méthodes de classification conventionnelles est que la précision de la classification d'utilisation du sol peut diminuer tandis que la quantité de l'information dans l'image augmente avec la résolution spatiale (Townshend, 1981; Irons *et al.*, 1985; Cushnie, 1987). Cela est dû à une augmentation de la variabilité spectrale dans les classes, causée par un nombre plus élevé d'éléments discernables de sous-classes, ce qui est inhérent à des données de résolutions spatiales plus détaillées et plus élevées (Shaban and Dikshit, 2001).

Les méthodes conventionnelles employées dans la classification des images multispectrales utilisent la signature spectrale de l'image. Cela est acceptable dans la segmentation des classes d'objets qui sont spectralement homogènes puisqu'il est possible de tracer des sites d'entraînement assez propres et représentatifs. Cependant, les résultats obtenus à partir de telles méthodes se caractérisent souvent par une précision limitée et une faible fiabilité

(Haala and Brenner, 1999), en particulier pour la cartographie des paramètres hétérogènes dans des scènes urbaines complexes. C'est parce que le potentiel d'information spectrale est limité puisque les objets urbains sont distingués mieux par leurs propriétés spatiales, autrement appelé texture, plutôt que leurs propriétés spectrales (Zhang, 1999).

Plusieurs chercheurs ont étudié la texture pour l'amélioration des classifications spectrales du milieu urbain (Conners *et al.*, 1984), mais on n'a pas encore étudié l'application de cette approche sur des images de haute résolution spatiale, telles que les images IKONOS. Donc, le but de ce projet de recherche est d'évaluer l'apport de la texture à la classification urbaine des images haute résolution spatiale afin de produire des résultats plus précis et d'extraire des données plus détaillées.

Les hypothèses proposées par cette étude sont :

- Les canaux de texture combinés avec les canaux spectraux peuvent fournir une classification plus précise des images de haute résolution IKONOS, particulièrement si les classes d'intérêt ne peuvent pas être distinguées l'une de l'autre en utilisant seulement des valeurs de niveau de gris, à cause de la nature hétérogène des objets urbains.
- Les images de haute résolution IKONOS peuvent produire des données plus détaillées de couverture du sol et d'utilisation du sol du milieu urbain par rapport aux images de résolution spatiale plus bas.

Les objectives de ce projet de recherche sont :

- Extraire les informations de texture de l'image panchromatique haute résolution spatiale IKONOS 1 x 1 mètre à partir de la méthode de l'analyse texturale de matrice de cooccurrence.
- Réaliser des classifications de couverture du sol et d'utilisation du sol des images IKONOS par la technique de classification de maximum de vraisemblance.
- Évaluer l'apport de la texture aux classifications.

La région d'étude pour ce projet de recherche couvre la section principale de la vieille ville de Sherbrooke, qui est située dans la zone sud de la province du Québec, Canada. Le centre

d'intérêt est composé de divers types d'utilisation du sol, tel que réseau routier, agriculture, résidentiel, commercial, industriel, institutionnel, et recréation, et de couverture du sol, comme rivière, sol nu, pelouse, arbustes, et forêt, ce qui fournit une bonne zone d'étude pour l'analyse de la classification urbaine.

Des images de haute résolution spatiale du satellite IKONOS-2 de Space Imaging ont été choisies pour ce projet de recherche. Les scènes satellitaires bruts sont multispectrale et panchromatique de 16 bits, avec une dimension d'image d'environ 11800 x 13200 pixels, acquis le 20 mai, 2001 à 10:50, heure locale. La projection de carte est le Mercator Transverse Universelle (UTM) et les paramètres spécifiques sont: hémisphère nordique, zone 18, NAD83. Pour les résolutions spatiales et spectrales des images voir le tableau 1.

Pour réaliser les objectives de cette étude, une méthodologie a été formulée sur les deux éléments principaux de cette recherche : l'analyse texturale et la classification spectrale-spatiale (voir la figure 3).

Pour l'étape de l'analyse texturale de cette étude, la méthode de la matrice de cooccurrence (Haralick *et al.*, 1973), a été utilisée. Il y a quatorze différents paramètres de texture qui peuvent être extraites de ces matrices. Le succès de la méthode de la matrice de cooccurrence dépend de la sélection appropriée de trois éléments : la distance entre les pixels, la direction entre les pixels, et la taille de la fenêtre.

La distance entre les pixels le plus souvent choisie est égale à 1 pixel; on l'a utilisée dans cette étude puisqu'elle est appropriée autant pour les textures fines que pour celles qui sont grossières. Pour cette étude la direction de 0° entre les pixels, qui est le choix le plus répandu dans la littérature, a été utilisée par défaut du système de traitement d'image.

La précision de la classification avec les paramètres de texture dépend aussi de la taille de la fenêtre utilisée. Si la fenêtre est trop petite ou trop grande par rapport à la structure texturale, les paramètres ne refléteront pas les vraies caractéristiques du texture (Mather *et al.*, 1998). Pour choisir la taille de la fenêtre, le coefficient de variation pour un paramètre donné est calculé pour chaque classe en fonction de la taille de la fenêtre (Laur, 1989). La taille de la fenêtre appropriée est celle pour laquelle la valeur du coefficient de variation commence à se stabiliser pour la majorité des classes, tout en ayant la valeur la plus basse.

Dans cette étude, le coefficient de variation a été calculé pour le paramètre homogénéité, qui a été choisi arbitrairement, en fonction de la taille de la fenêtre pour chaque classe. Les résultats ont démontré que le coefficient de variation a commencé à se stabiliser à la taille de la fenêtre de 11x11 pixels pour la majorité des classes.

Il faut choisir les paramètres de texture qui sont les plus utiles pour l'étude car plusieurs d'entre eux présentent des redondances. Par défaut, le système de traitement d'image permet d'employer seulement huit paramètres de texture : contraste, corrélation, dissimilarité, entropie, homogénéité, moyenne, second moment, et variance. À partir de l'image panchromatique, des néo-canaux de texture des huit paramètres différents ont été produits en utilisant une fenêtre mobile 11x11, qu'on a trouvé la plus appropriée, et avec la direction de 0° et la distance de 1 pixel entre les pixels.

Les paramètres les plus utiles pour une bonne discrimination de classe urbaine ont été choisis à l'aide des étapes suivantes : l'analyse de la qualité visuelle des images de textures (voir la figure 7), l'affichage des histogrammes de tous les canaux (voir la figure 8), et le calcul de la matrice de corrélation (voir le tableau 2). Le résultat de ces étapes était la sélection des paramètres suivant : moyenne, homogénéité et dissimilarité.

La technique de classification par le maximum de vraisemblance est la plus populaire et extensivement utilisée parmi toutes les autres méthodes de classification dirigées (Mather *et al.*, 1998); elle calcule la plus grande probabilité qu'un pixel appartient à une classe donnée, ainsi réduisant les fausses classifications des pixels au minimum. C'est la technique qu'on a employée pour l'étape de la classification dans cette étude.

La méthode la plus répandue pour l'intégration des données de texture avec les données spectrales consiste à utiliser les données de texture comme des canaux de texture à combiner avec les canaux spectraux dans le processus de classification (Marceau *et al.*, 1990; Coulombe *et al.*, 1991). Dans cette étude, les images d'entrée qu'on a intégrées ont été mises en trois groupes: un groupe de données des quatre images multispectrales (rouge, vert, bleu et proche-infrarouge), un groupe de données spatiales des trois images de texture (moyenne, homogénéité et dissimilarité) qu'on a produit à partir des étapes du processus de l'analyse texturale, et un groupe de données combinées composé des deux groupes de données spectrales et spatiales. Le processus de classification a été réalisé pour chaque groupe de données.

L'étape finale de la classification est l'évaluation de la précision des résultats obtenus. Une fois que l'espace spectral est segmenté en régions différentes associées à chaque classe d'objet, les pixels dans les sites de vérification sont assigné l'étiquette de la classe qui les représente dans l'espace spectral segmenté. Le résultat global de ce processus est présenté dans une matrice de confusion. À partir de cette matrice plusieurs indices de précision de la classification peuvent être calculés. Puisque le coefficient de Kappa est l'indice le plus approprié pour fournir une évaluation exacte de la classification, parce qu'il tient compte de tous les éléments de la matrice de confusion (Fung and Ledrew, 1988), c'est la méthode qu'on a adoptée dans cette étude. Les précisions des résultats de la classification des trois groupes de données sont présentées dans le tableau 4.

Les résultats obtenus par cette étude ont démontré que la classification faite uniquement avec le groupe de données spatiales (les canaux de texture moyenne, homogénéité et dissimilarité) a produit des précisions s'étendant de 59.8 % à 84.9 % pour toutes les classes, avec une précision globale de 73.5 %. La classification du groupe de données exclusivement spectrales (les canaux rouge, vert, bleu et proche-infrarouge) a produit des précisions un peu plus élevées comparées au groupe de données spatiales, s'étendant de 62.4 % à 87.5 % pour toutes les classes, avec une précision globale de 78.9 %. Les précisions les plus élevées obtenues dans cette étude sont avec la classification de la combinaison des groupes de données spectrales et spatiales, qui a produit des précisions s'étendant de 70.6 % à 90.9 % pour toutes les classes et une précision globale de 86.1 %, ce qui indique une amélioration globale de 7.2 % par rapport au groupe de données spectrales.

Ces résultats ont montré qu'avec la combinaison des données spectrales et spatiales, les précisions de la classification urbaine sont les plus élevées. Donc, les résultats soutiennent l'hypothèse formulée pour cette étude que l'application des canaux de texture combinés avec les canaux spectraux aux images de haute résolution IKONOS peut produire des classifications plus précises et des données urbaines plus détaillées.

TABLE OF CONTENTS

LIST OF FIGURES

LIST OF TABLES

LIST OF APPENDICES

ACKNOWLEDGMENTS

I would like to gratefully acknowledge the valuable assistance and advice provided throughout this research project and in the writing of this thesis by my director Dr. Dong-Chen He, as well as the support, confidence and encouragement shown by my co-director Dr. Goze Bertin Bénié.

I greatly appreciate the helpful discussions and suggestions of Dr. Hassan Anys, as well as the aid of various professors, colleagues and personnel at the Centre d'Applications et de Recherches en Télédétection (CARTEL) of the University of Sherbrooke.

In particular, I would like to express my deep gratitude to Dr. Kamel Soudani, whom I had the great fortune to work with at CARTEL, and whose scientific collaboration, interesting discussions, and insightful critique were instrumental to the successful completion of this project.

CHAPTER 1

Introduction

1.1 Thesis Overview

The term "remote sensing" means the acquisition of measurements of specific objects from a distance. Early remote sensing consisted of measuring objects and their properties on the surface of the earth through photo-interpretation of aerial photographs. In the modern study of remote sensing, this is accomplished through the use of data obtained from sensors onboard airborne or space borne vehicles, such as aircraft and satellites.

Remote sensing systems provide valuable information that can be applied to a wide range of fields. One significant application of this technology is to the domain of environmental and land assessment, which deals with such areas as urban planning and management, land cover and land use monitoring, etc. This is an important field of study because the principal factor involved is the ever-increasing human population.

A variety of remote sensing systems are available that provide data based on various parameters, such as spatial resolution, spectral resolution, and temporal resolution, to suit the needs of different users. The development of high spatial resolution sensors makes remote sensing data a highly potential source of detailed urban land cover and land use information. However, techniques used to process these images to extract the desired information have to keep up with the changing technologies. As spatial and spectral resolutions of the remote sensor systems increase, image processing algorithms have to be developed in order to determine how to exploit the raising volume of data as efficiently as possible.

It is in this perspective that the present research study was undertaken. Given that conventional image classification methods based solely on spectral data have proven to be inadequate for high-resolution imagery, this study focuses on the contribution of texture, which is based on spatial information within the image, for the discrimination of urban objects. Two useful and commonly used image processing techniques, the Grey Level Co-occurrence Matrix

texture analysis and the Maximum Likelihood multispectral classification, are evaluated as a combined approach for the extraction of urban land cover and land use information from high spatial resolution IKONOS satellite scenes.

1.2 Scientific and Practical Importance and Contributions

As demands for better land management and urban monitoring increase due to an exponentially growing global population, land use and land cover information is proving to be a very significant source of data. Urban land use and land cover are dynamic and change rapidly with time. To keep this information up-to-date, the current land use status needs to be surveyed periodically. In the past, this information was usually extracted from aerial photography, which is a costly and time-consuming process.

The arrival of digital remote sensing images has made way for more automated extraction of urban information. Land cover and land use data derived through computer algorithms provide more quantitative details that are not possible to obtain through human analysis. As a result, the availability of IKONOS images at higher spatial resolutions is causing gradual improvements in urban interpretation and classification, and is becoming a real alternative to aerial photography (Leckie *et al.*, 1995; Stoney and Hughes, 1998; Anger, 1999).

The aim of this thesis is to contribute to the understanding of how to effectively derive more accurate urban data from higher spatial resolution imagery, which will lead to improved automated classification procedures that will help to overcome the obstacles in obtaining current detailed urban land cover and land use information.

CHAPTER 2

Theoretical Framework

2.1 Problematic

Land use and land cover information is constantly changing as a result of an increasing human population. Due to conflicting land use demands, this type of information is very important in different urban applications, such as urban planning. As pressures increase for better land management, high-resolution satellite imagery is proving to be very promising in providing more detailed urban land cover and land use data. However, both public and private organizations are in need of effective and efficient tools for the exploitation of these images.

The terms "land use" and "land cover" are often used interchangeably as well as incorrectly. Land use refers to human employment of the land and is of interest mostly to social scientists. Land cover deals with the physical state of the land and is the affair primarily of natural scientists (Turner and Meyer, 1994).

In general, there are two types of land cover changes: land cover conversion and land cover modification. This is an important, although largely unrecognized distinction that has significant implications for satellite image analysis. Land cover conversion concerns a shift in the relative proportions of land cover classes within a given area, such as urban expansion into formerly agricultural land, or clear cutting of forests for transformation into croplands or pastures. It is land cover conversion that has received most notice, as it tends to be more localized and immediate in impact and, therefore, draws greater attention. Land cover modification involves a shift within a particular land cover class, such as tree thinning on forested land. Land cover modification tends to occur more gradually and over a wider area, making it more difficult to perceive, but no less important (Turner and Meyer, 1994).

Satellite images are objective and spatially comprehensive. As a result, they are very useful for characterizing land use and land cover. Changing settlement patterns in both urban landscapes (Lo and Shipman, 1990; Pathan *et al.*, 1993) and rural landscapes (Nellis *et al.*, 1990;

Dimyati *et al.*, 1996) are just examples of the many land use change processes, which have been successfully quantified through remote sensing data (Hudak and Wessman, 1998).

The application of remote sensing imagery for future urban planning is thus a very sensible as well as indispensable choice. Arguments in favour of the use of satellite systems are: fast data access, quick visual interpretation, good representation on a planar surface, and great cartographic representation after the process of geometrical correction. A further advantage is the wide range of possible applications of the qualitative and quantitative image classifications, such as the analysis of urban boundaries, layout structures, and building densities (Balzerek, 2001).

Since the launch of the IKONOS satellite in 2000, satellite images with higher ground resolutions are available, causing gradual improvements in urban interpretation and classification (Balzerek, 2001). Especially in urban planning, high spatial resolution multispectral imagery, such as those captured by the sensor on the IKONOS-2 satellite, are becoming a real alternative to aerial photography (King, 1995; Roberts, 1995; Caylor *et al.*, 1999; Green, 2000; Moskal and Franklin, 2001). A much greater amount of information can be extracted from this imagery than from the previous generation of satellite data, which typically had 10 - 100 meter pixel resolutions.

Among commercial satellite sensors, IKONOS has state-of-the-art radiometric, spatial, and temporal resolutions in four traditional spectral bands. With the increasing availability of imagery at these resolutions, there is an expanding need for automated feature extraction. Artificial intelligence systems are being created to extract specific user-defined features such as buildings, roads, and other land use classes from high-resolution imagery. These classes often differ from their associated land cover materials and therefore from their per-pixel spectral signatures. As a result, traditional classification methods, which were developed in the era of 10 – 100 meter pixel resolution satellite scenes, are not suitable for higher-resolution imagery (Barr and Barnsley, 1997).

A significant drawback of these conventional spectral-based, per-pixel classification approaches is that while the information content of the imagery increases with spatial resolution, the accuracy of the land use classification may decrease (Townshend, 1981; Irons *et al.*, 1985; Cushnie, 1987). This is due to a higher number of detectable sub-class elements resulting in

increasing spectral variability within the classes, inherent in more detailed, higher spatial resolution data (Shaban and Dikshit, 2001).

The use of spectral classification techniques for analyzing and mapping the urban environment presents a few other major obstacles. One is that landscapes are composed of natural and artificial materials that sometimes present close or even identical spectral properties, which can introduce important confusion between classes. This confusion can also be caused by the fact that groups of pixels representing the same land cover type will not necessarily have the same spectral information due to noise in the data, atmospheric effects, and natural variation within the land cover type (Smith and Fuller, 2001).

Another is that in urban environments, many of the classes of interest are made up of a collection of diverse features. For example, residential areas are typically seen from above as a mixture of tree crowns, rooftops, lawns, paved streets, driveways and parking lots. It is the composite of these features, rather than an inventory of the individual components, that is often of interest. Operationally, a method is desired that focuses on the pattern of variation, defined by characteristics such as texture, shape, size and orientation, rather than or in addition to, the individual pixel brightness. Human interpreters can do this easily, but it is still problematic to get an automated process to perform the task adequately (Campbell, 1987).

Conventional approaches used in the classification of multispectral imagery basically employ the spectral signature of the image. This is acceptable in the segmentation of spectrally homogeneous object classes since it is possible to delineate fairly clean and representative training sites. Results obtained from such methods though, are unsatisfactory, particularly in the case of applications involving the mapping of heterogeneous features in complex urban scenes. In general, these results are often characterized by limited accuracy and low reliability (Haala and Brenner, 1999). This is mainly because the potential of spectral information is limited since urban objects are distinguished better through their spatial properties rather than their spectral properties (Zhang, 1999; Kiema, 2002).

Many have investigated texture and other spatial frequency patterns as possible sources of unique information to supplement pixel-based spectra (Jensen, 1996). A potential approach to overcome the obstacles of spectral classification of high-resolution imagery is to integrate spatial

data into the classification process. Texture features have been previously used on remote sensing images of urban environments with varying degrees of success (Conners *et al.*, 1984). However, land cover classification algorithms based on image spatial characteristics, known as texture, have never been as popular as spectral-based algorithms, although significant progress has been made in using textural analysis to improve spectral classifications of satellite data (Franklin and Peddle, 1989; Franklin and Peddle, 1990; Møller-Jensen, 1990; Agbu and Nizeyimana, 1991; Kushwaha et al., 1994; Hay *et al.*, 1996; Ryherd and Woodcock, 1996; Hudak and Wessman, 1998).

The texture study is based on the analysis of the spatial distribution of the local tonal variations (Holecz *et al.*, 1993) that is able to point out linear structures of a remotely sensed image, which can be used to characterize phenomenon such as urban morphology (Ober *et al.*, 1997). Both aerial photograph interpreters (Avery and Berlin, 1992) and digital image analysts (Franklin and McDermid, 1993; Jakubauskas, 1997; Bruniquel-Pinel and Gastellu-Etchegorry, 1998) have long since recognized image texture as a powerful source of information in urban remote sensing analysis (Moskal and Franklin, 2001). However, the application of textural approaches to high spatial resolution imagery, such as those captured by the IKONOS satellites, for the extraction of urban data has yet to be studied.

2.2 Hypothesis

- Texture channels can provide a more precise classification of high-resolution IKONOS imagery when combined with spectral channels, especially if the classes of interest cannot be distinguished from each other by using grey-level values alone, due to the heterogeneous nature of urban objects.

- High spatial resolution IKONOS imagery can produce more detailed land cover and land use data of the urban environment compared to lower spatial resolution images.

2.3 Objectives

- To extract textural information from high spatial resolution IKONOS panchromatic 1 x 1 meter imagery through the textural analysis method of the Grey Level Co-occurrence Matrix.

- To perform urban land use and land cover classifications of the IKONOS imagery using the Maximum Likelihood Classification technique.

- To evaluate the performance of the classifications involving spatial data.

CHAPTER 3

Texture Analysis

3.1 Introduction

Each and every grain in any object has a different crystallographic orientation. However, preferred orientation, which is known as texture and is described by the spatial distribution of the local tonal variations in a scene, is what is usually observed. Textures can be found in abundance in the visual world, at all scales of perception. As soon as there is enough detail in an adequate visual angle, a texture becomes distinguishable.

Humans have a powerful innate ability to recognize textural differences. Although the complex neural and psychological processes by which this is accomplished have so far evaded detailed scientific explanation (Hay *et al.*, 1996), studies concerning texture perception by the human visual system have provided useful insights into the importance of textural information, as well as the complex nature of texture discrimination.

These notions are very significant in the study of texture analysis, which deals with various techniques for modeling textures and extracting texture features that can then be applied to such tasks as, classification, segmentation, texture synthesis and shape extraction. The concepts of human texture perception are meaningful to other fields as well, such as image processing and pattern recognition (Julesz and Bergen, 1983), which attempt to solve problems involving visual data through the use of texture.

A very common method used in discriminating objects is pattern recognition. In order to recognize different types of objects in the visual world, we can use the texture of an object that has its own specific visual pattern as an indication. According to Pickett (1970), the basic requirement for an optical pattern to be seen, as texture, is that there be a large number of elements (spatial variations in intensity or wavelength), each to some degree visible, and, on the whole, densely and evenly arrayed over the field of view.

Texture analysis is one of the most important techniques used in image processing and pattern recognition, mainly because of the fact that it can provide information about the arrangement and spatial properties of image fundamental elements. Such textural information is complementary to multispectral analysis of images and is sometimes the only way in which a digital image can be characterized. A good understanding or a more satisfactory interpretation of an image should, therefore, include the description of both spectral and textural aspects of the image (He and Wang, 1991).

In fact, Haralick *et al.* (1973) demonstrated this concept through their studies, which showed that spectral classification precisions of an image could be increased with the integration of textural data. This conclusion caused texture analysis to become an extremely interesting field of research, especially for applications in remote sensing. However, proposed methods were difficult to apply or had limited applications due to the low spatial resolution of the satellites at that time (Kiema, 2002), and due to inadequate computer capacity.

Over the last few years, though, the latest remote sensing technology has greatly advanced in the areas of spatial and spectral resolution. Along with the significant improvements in digital processing and increased computer capabilities, the study of texture analysis is once again booming with research interest.

Since texture plays one of the dominant roles in all types of images, from remotely sensed, biomedical, and microscopic images to printed documents, texture analysis has a very wide range of practical applications that are useful to a variety of domains, from mature fields, such as remote sensing to more recent disciplines, such as automated inspection and document processing. As a result, the importance of research in the area of texture and its analysis is quite evident.

3.2 Definition of Texture

What is texture? Everyday texture terms - rough, silky, bumpy - refer to touch, but what about the textures that we sense visually? Even though we easily recognize texture when we see it, describing texture in words can be very difficult. This difficulty can be well understood by the number of different texture definitions that researchers have attempted to develop. Coggins

(1982) has compiled a catalogue of texture definitions from computer vision literature, some examples of which are given here (Tuceryan and Jain, 1998):

- We may regard texture as what constitutes a macroscopic region. Its structure is simply attributed to the repetitive patterns in which elements or primitives are arranged according to a placement rule (Tamura *et al.*, 1978).
- A region in an image has a constant texture if a set of local statistics or other local properties of the picture function are constant, slowly varying, or approximately periodic (Sklansky, 1978).
- The image texture considered is non-figurative and cellular... An image texture is described by the number and types of its (tonal) primitives and the spatial organization or layout of its (tonal) primitives... A fundamental characteristic of texture: it cannot be analyzed without a frame of reference of tonal primitives being stated or implied. For any smooth grey-tone surface, there exists a scale such that when the surface is examined, it has no texture. Then as resolution increases, it takes on a fine texture and then a coarse texture (Haralick, 1979).
- Texture is defined as an attribute of a field having no components that appear enumerable. The phase relations between the components are thus not apparent. Nor should the field contain an obvious gradient. The intent of this definition is to direct the attention of the observer to the global properties of the display — i.e., its overall "coarseness," "bumpiness," or "fineness." Physically, non-enumerable (a-periodic) patterns are generated by stochastic, as opposed to deterministic, processes. Perceptually, however, the set of all patterns without obvious enumerable components will include many deterministic (and even periodic) textures (Richards and Polit, 1974).
- Texture is an apparently paradoxical notion. On the one hand, it is commonly used in the early processing of visual information, especially for practical classification purposes. On the other hand, no one has succeeded in producing a commonly accepted definition of texture. The resolution of this paradox will depend on a richer, more developed model for early visual information processing, a central aspect of

which will be representational systems at many different levels of abstractions. These levels will most probably include actual intensities at the bottom and will progress through edge and orientation descriptors to surface, and perhaps volumetric descriptors. Given these multi-level structures, it seems clear that they should be included in the definition of, and in the computation of, texture descriptors (Zucker and Kant, 1981).

- The notion of texture appears to depend upon three ingredients: (i) some local 'order' is repeated over a region which is large in comparison to the order's size, (ii) the order consists in the non-random arrangement of elementary parts, and (iii) the parts are roughly uniform entities having approximately the same dimensions everywhere within the textured region (Hawkins, 1969).

- Texture appears as the tonal patterns of an image-object resulting from the spatial arrangement of the three dimensional object's reflective surfaces. Image-object is the two-dimensional projected image of a three-dimension real world object, whose intensity values depend on (i) the geometry of the physical object (ii) the reflectance of the visible surfaces (iii) the illumination of the scene and (iv) the viewpoint of the observer (Marr, 1982).

As we can see from this collection of descriptions, different people define texture depending upon its particular application, thus there is no generally agreed upon definition. Some definitions are perceptually motivated; others are based completely on the application in which it will be used.

For applications in remote sensing, texture is generally described as the group of relationships between grey levels of neighbouring pixels that contribute to the overall appearance and visual characteristics of an image. This description takes into account the forms and periodicities contained in the image. There exists, however, a problem concerning this definition; it does not provide a rigorous mathematical description for texture with which a quantitative evaluation of textures present in natural images can be made. Most definitions that have been developed simply enumerate the properties and causes of texture.

With this in mind, Haralick *et al.* (1973) proposed the texture definition that images are represented by the spatial distribution of objects of a specific size and having reflectance or emmitance characteristics. The spatial organization and the relationships between these objects correspond to the spatial distribution of grey levels in the image. Thus, texture can be considered as the pattern of the spatial distribution of grey levels. Haralick (1979) later took this definition further and suggested a more structural description, where texture is a spatial occurrence that is based on two aspects: primitives, which are groups of pixels that are related and characterized by certain attributes, and their laws of configuration, which govern their arrangement throughout the image.

One important factor that is usually overlooked in the definition of texture, however, is the scale of observation, or resolution, at which the texture is viewed. This is significant because texture is a complex multiscale phenomenon (Ahearn, 1988); it has a recursive nature. A primitive at one scale may contain a micro-texture composed of primitives defined at a smaller scale. For example, consider the texture represented in a brick wall. When viewed at a low resolution, the texture of the wall is perceived as formed by primitives, which are individual bricks. When viewed at a higher resolution, texture is perceived as the details present in each individual brick.

As a result, Laws (1980) accounted for this element and developed the following description: texture is that which remains constant when a window is moved across the image, but that can change according to the size of the window. This definition, however, is based on the assumption that the image contains only one texture.

Since the perception of texture is dependent on the observer, Laws formed an additional definition to explain for this factor. If two regions with the same texture have a difference in brightness, contrast, colour, size, rotation or geometric distortions, most observers will still consider these two regions to have the same texture even though they have a distinguishable difference. Thus, texture does not exhibit any important variation when subject to translation. Therefore, according to Laws, texture is perceived as being invariant to translation.

Unser (1984) formulated a more complete definition of texture founded on the significance of the human visual system in texture perception. He suggested the definition that

texture is an area of an image for which there is a window of reduced size, such that an observation through it results in the same visual perception for all possible translations, within the area of interest. Based on this, Slimani (1986) also suggested that all texture definitions should encompass important insights on texture perception, as well as a realistic model of our visual system (Anys, 1995).

3.3 Human Texture Perception

The human visual system is so expert at handling textural details that we are rarely conscious of the way in which textural information is used in understanding our visual environment. As a result, people generally have a natural idea of what texture means to them. The exact processes through which we identify or discriminate textures, however, are still not known. Thus, the psychophysics of texture perception continues to be a subject of intense interest.

Take the example of a tiger in the forest. The detection of a tiger among the foliage is a perceptual task that carries life and death consequences for someone trying to survive in the forest. The success of the tiger in camouflaging itself is a failure of the visual system observing it. The camouflage is successful because the visual system of the observer is unable to discriminate the two textures: the foliage and the tiger skin. This type of discrimination can be based on various cues such as brightness, form, colour, texture, etc. How these cues are used and what the visual processes are form the basis of the study of texture perception by psychologists (Tuceryan and Jain, 1998).

Many researchers have speculated about the mechanisms involved in visual texture perception, and conducted studies that have provided some important theories on the subject. These theories are useful, particularly for applications in texture analysis, because they offer ideas about what image properties are needed for human texture perception that can be used to develop mathematical models, or to improve existing ones, for automated processes. At the least, these theories can serve as a reference against which proposed computer algorithms for texture analysis can be evaluated. Although most early theories developed for the explanation of human texture perception are basically not very different from one another, some of them have their own unique speculations, which stress the complexity of this impressive phenomenon.

3.3.1 The Julesz Paradigm

One psychophysicist who has studied texture perception by the human visual system extensively in the context of texture discrimination is Julesz. Through his pioneering work, he developed many theories, which he continually enhanced, in an effort to explain the elusive processes of human texture vision.

From his early studies, Julesz (1962) found that texture discrimination by the human visual system appears to be accomplished without the use of high-level cognitive processes. He also found that random dot textures with different statistical properties are effortlessly distinguishable. This fact prompted him to the hypothesis that in general, texture discrimination is based on a very low-level perceptual mechanism that performs a statistical analysis of intensities in texture fields.

Texture patterns can be characterized by the joint probability distributions of their intensities. These distributions, or their statistics, have associated orders of density:

- First-order (monopole) statistics measure the probability of observing a grey value at a random location in the texture field of the image. They are derived from the one-dimensional frequency of occurrence (histogram) of pixel intensities. These depend only on individual pixel values and not on the interaction or co-occurrence of neighbouring pixel values.
- Second-order (dipole) statistics are derived from the probability of observing a pair of grey values occurring at the endpoints of a dipole of random length placed in the texture field of the image at a random location and orientation. These are properties of pairs of pixel values.
- Third-order (tripole) statistics are derived from the probability of observing intensity triplets occurring at the vertices of an arbitrary triangle, randomly placed in the texture field of the image.

Julesz discovered that textures with different first-order statistics are effortlessly distinguishable due to perceived average brightness, contrast, etc. He found that textures with equal first-order statistics but different second-order statistics are also easily distinguishable due

to perceived differences in granularity. However, Julesz could not find any examples of textures with equal first-order and second-order statistics, but different third-order statistics that are easily distinguishable. He therefore hypothesized that textures are not easily, or preattentively, distinguishable if their second-order statistics are identical, such as the texture pair in Figure 1(a). Thus, he concluded that second-order statistics are sufficient for human texture perception.

Julesz proved that his conjecture was valid through subsequent studies (Julesz *et al.*, 1973; Julesz, 1975). Contrarily though, he found a few counterexamples to his theory. Julesz discovered a set of:

- Textures with equal second-order statistics, which are preattentively discriminable based on the perceived local geometrical features of collinearity, corner, and closure of micro-patterns, seen in the texture pair in Figure 1(b).
- Textures with identical third-order statistics that are easily distinguishable based on perceived differences in granularity.
- Textures that have different second-order statistics, which are not effortlessly discriminable.

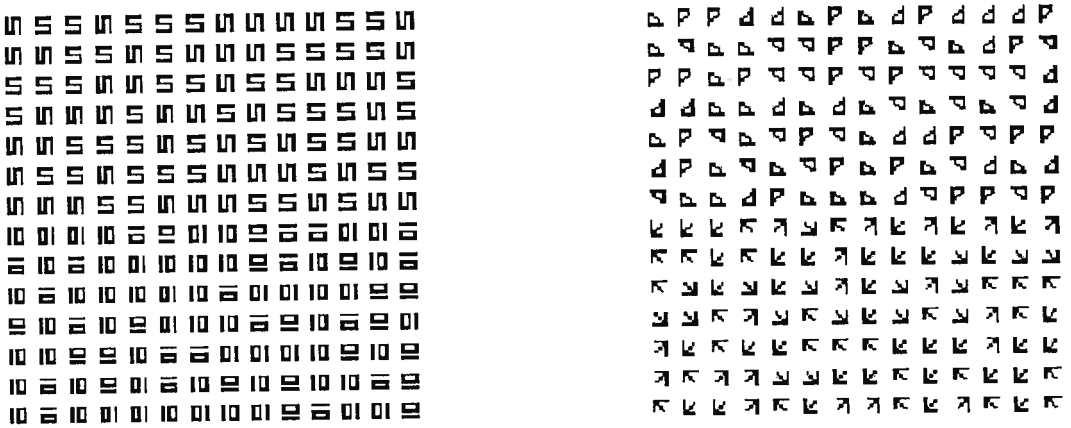

(a) (b)

Figure 1: Texture Pairs with Equal Second-order Statistics. The lower halves of the images contain different texture tokens than the top halves. (a) The two textures are not easily discriminable. (b) The two different textures are effortlessly detectable (Tuceryan and Jain, 1998).

Other researchers considered Julesz's experiments to be inadequate due to the fact that the textures used in his experiments had many limitations. For example, the textures only contained four grey levels, and they were generated line by line, having no vertical correlation, whereas all natural textures do. In an effort to rectify this, Pratt *et al.* (1978) conducted further studies on the same theme, with full control over the number of grey levels and spatial correlations of the textures used, which allowed them to experiment with samples that are closer to natural textures. Their results confirmed the Julesz conjecture, but could not account for the counterexamples found by him.

In order to explain the inconsistency of his initial hypothesis, Julesz developed a paradigm for human texture perception that is based on two mechanisms. The first uses low-level detectors to calculate differences in second-order statistics of image intensities. The second extracts first-order statistics of local image features using simple feature detectors. The two mechanisms work independently, and if the first mechanism does not find much difference in second-order statistics, discrimination through the second mechanism may still be accomplished.

Based on the Julesz paradigm, Schatz (1977) conducted studies in order to establish what amount of full second-order statistics is needed for preattentive texture detection by the human visual system. He found that effortless discrimination of textures with different second-order statistics is dependant on a restricted set of statistics. This was determined by experimenting with textures generated by line and point primitives that have a set of statistics based on dipoles placed on actual lines in the texture as well as on virtual lines between termination points, such as corners, end points, isolated points, etc. Schatz concluded that the restricted set of statistics seem to be necessary and, perhaps sufficient for preattentive texture detection.

3.3.2 The Primal Sketch Paradigm

Since Julesz himself has developed an alternate theory for texture vision that is different from his original conjecture, other researchers, such as Marr, have opposed the Julesz conjecture. Instead, Marr (1976) proposed a paradigm for human texture perception that is described by the primal sketch, where texture discrimination is based on the calculation of first-order statistics of primal sketch primitives, as well as on the processes which group these primitives.

The primal sketch is a symbolic representation of an image, correlated with edge and bar masks of various sizes and directions to detect primitives, such as edges, lines, and blobs, having attributes such as, orientation, size, contrast, position and termination points. These primitives are representative of specific local image features, and according to Marr, they characterize all of the useful information in an image.

If the processes used for grouping these primal sketch primitives perform adequately, then Marr's theory seems more adept at extracting significant textural information from an image than the Julesz paradigm. However, the primal sketch paradigm does not provide a detailed explanation concerning these grouping processes.

Many researchers have studied the involvement of perceptual grouping in texture discrimination. Studies conducted by Beck (1983) found that texture perception through grouping that is based on similarity, is effortless and appears to depend on simple elements in the image such as direction of lines, size, and brightness. In later studies, Beck *et al.* (1987) counter that discrimination of some specific textures is mainly based on the analysis of spatial frequency rather than on higher-level symbolic grouping. Zucker and Cavanaugh (1985) performed experiments that show how texture perception can be accomplished through the grouping of subjective features in a texture field.

3.3.3 Other Models for Human Texture Detection

From the perspective of Laws (1980), the human visual system employs certain mechanisms, such as contour detection, for extracting qualitative textural information from images independently of its source. Transformations in the retina of the human eye conserve as much information as possible in order to discriminate different textures, as well as to overlook information that may cause two identical textures to appear different.

Texture can be described by its various apparent qualities. As many as ten different textural qualities have been identified by Laws for this purpose: uniformity, density, coarseness, roughness, regularity, linearity, directionality, direction, frequency, and phase. However, Laws has not provided details about the mechanisms used by the human eye, and how these qualitative characteristics of texture are processed in the discrimination of texture.

Further studies conducted by Julesz (1981a, 1981b) resulted in the "theory of textons" as an improved model for texture perception. Textons are described as visual occurrences, such as collinearity, closures, terminations (endpoints of line segments or corners), etc., that are detected by the visual system and then used to discriminate texture. For example, the two textures in Figure 1(a) have the same number of terminations; the texton information is the same, therefore, preattentive discrimination of the texture pair is not possible. In Figure 1(b), the texture in the upper half has a different number of terminations than the texture in the lower half, resulting in a difference in texton information thus making the texture pair distinguishable.

Later on, Julesz and Bergen (1983) extended the texton theory to produce a model for preattentive texture discrimination. By using textures with differing texton information, they described how the visual system operates in two modes: the attentive mode and the preattentive mode. In the process of texture detection, human vision in the preattentive mode instantly covers a large zone in a parallel manner, whereas in the attentive mode, smaller zones are covered in sequence. Vision in the attentive mode is directed towards zones containing differences in textons that are detected by vision in the preattentive mode.

3.3.4 Contributions of Psychophysics to Texture Analysis

The different theories presented by psychophysics researchers over the years have provided many clues that have supported and aided the formation of mathematical models for the quantitative analysis of texture. In the field of remote sensing, some of these models have already been applied with varying degrees of success.

For example, several ideas extracted from studies done by Julesz, as well as other research based on the same theme, emphasize the value of statistical methods of texture analysis, especially those of second-order statistics, such as the grey level co-occurrence matrix. Concepts generated by Marr's research verify the importance of structural elements in the texture study of images, and support approaches that calculate statistics based on more complex local features rather than simple intensities.

3.4 Texture Analysis in Remote Sensing

Texture analysis techniques can generally be divided into two broad categories: structural methods and statistical methods (Haralick, 1979; Sali and Wolfson, 1992). Structural methods of texture analysis consider texture to be composed of texture primitives that are arranged according to a specific placement rule. Different types of primitives, their orientation and shape, along with other properties are considered to determine the appearance of texture. This type of analysis includes the extraction of texture primitives in the image, shape analysis of the texture primitives, and estimation of the placement rule of the texture primitives. Structural texture analysis approaches can derive much more detailed textural information and are generally used for the analysis of coarse macro-textures (Tomita and Tsuji, 1990).

Statistical textural analysis computes parallel local features at each point in a texture image, and derives a set of statistics from the distribution of these local features. The local feature is defined by the combination of intensities, or grey-levels, at specified positions relative to each point in the image. According to the number of points that define the local feature, statistics are classified into first-order, second-order, and higher-order statistics. Various texture features can then be extracted from these statistics. This type of analysis is usually employed for fine micro-textures (Tomita and Tsuji, 1990).

Texture is an important property of a reflective surface, which the human visual perception system uses to segment and classify image-objects in a two-dimensional image. If the proper image processing algorithms are developed, then the textural properties of remotely sensed images will provide valuable information for segmentation and classification techniques. In digital remote sensing, texture is considered to be the visual impression of coarseness or smoothness caused by the variability or uniformity of image tone (Avery and Berlin, 1992). According to Hay and Niemann (1994), texture in a digital forest scene is caused from the reflective variability of different structural vegetation patterns such as branching patterns, and crown sizes, shapes, and spatial arrangements.

Texture analysis has been extensively used to classify remotely sensed images. Structural analysis based on techniques such as the Fourier spectrum (Matsuyama *et al.*, 1980; D'Astous and Jernigan, 1984; He *et al.*, 1987), description of tonal primitives (Tomita *et al.*, 1982),

mathematical morphology (Chen and Dougherty, 1994; Li *et al.*, 1998; Pesaresi and Bianchin, 2001), cortex transform (Goresnic and Rotman, 1992), image filtering (Voorhees and Poggio, 1987; Blostein and Ahuja, 1989), and the medial axis transform (Tomita and Tsuji, 1990), have seen various applications. In remote sensing, however, the most common techniques used for texture analysis are usually statistical methods. This is mainly due to the fact that structural approaches are too complex for the analysis of landscape images where the spatial organization of objects is randomly regulated and more easily explained by the laws of probability (Marceau, 1988). Also, the structural texture primitives of natural scenes in satellite imagery are not easily identifiable (He and Wang, 1991; Shaban and Dikshit, 2001), and the description of their placement rules may be extremely complicated (Chellappa and Kashyap, 1985).

There are numerous statistical techniques based on the analysis of texture. The more common approaches are the Fourier transform (Wezska *et al.*, 1976), autocorrelation functions (Kaiser, 1995), semivariograms (Miranda *et al.*, 1996), grey level co-occurrence matrix (Haralick *et al.*, 1973; Haralick 1986; Haralick and Shapiro, 1992), grey level differences (Unser, 1986), texture spectrum (Wang and He, 1990), and textural signatures (Kourgli and Belhadj-Aissa, 2000). Among these techniques, the most popular statistical approach used for texture analysis is the grey level co-occurrence matrix (GLCM) (Kilpelä and Heikilä, 1990; Gong *et al.*, 1992).

3.5 Grey Level Co-occurrence Matrix Texture Analysis

A second-order histogram is an array that is formed based on the probabilities that pairs of pixels, separated by a certain distance and a specific direction, will have co-occurring grey levels. This array, or second-order histogram, is also known as the co-occurrence matrix. Use of co-occurrence matrices for the extraction of textural information from an image is based on the hypothesis that image texture can be defined by the spatial relationships between pixel grey levels of the image. Since the co-occurrence matrix expresses the two-dimensional distribution of pairs of grey-level occurrences, it can be considered a summary of the spatial and spectral frequencies of the image.

Let f be a rectangular, discrete image containing a finite number of grey levels. f is defined over the domain:

$$D = \{(i, j) : i \in [0, n_i), j \in [0, n_j), i, j \in I\} \quad (1.1)$$

by the relation:

$$f = \{((i, j), k) : (i, j) \in D, k = f(i, j), k \in [0, n_g), k \in I\} \quad (1.2)$$

where I denotes the set of integers, $\mathbf{n}_i$ and $\mathbf{n}_j$ are the horizontal and vertical dimensions of f, and $\mathbf{n}_g$ is the number of grey levels in f.

The grey level co-occurrence matrix (GLCM), **G**, is a square matrix of dimension $\mathbf{n}_g$ and is a function of both the image, f, and a displacement vector, d:

$$d = \{ [i, j] : (|i|, |j|) \in D, \| [i, j] \| > 0 \} \quad (1.3)$$

in the image plane (i, j), which constitutes the second-order spatial relation:

$$\mathbf{G}(f, d) = [g_{ij}(f, d)] \quad (1.4)$$

Each element $\mathbf{g}_{ij}$ of the matrix represents an estimate of the probability that two pixels separated by d have grey levels i and j.

Texture analysis based on the method of co-occurrence matrices rarely uses individual elements of the GLCM. Instead, statistical features are derived from the matrix for the extraction of textural information from the image. A large number of texture features have been proposed; as many as fourteen different features that can be derived from these matrices are described by Haralick *et al.* (1973), however, only some of these are widely used. This is because many of the features are redundant, due to their high correlation. Thus they are not all useful for describing a particular texture. Some of the texture features that can be extracted from the GLCM are as follows:

- Angular Second Moment
- Contrast
- Correlation
- Dissimilarity
- Entropy
- Homogeneity
- Mean
- Variance

3.5.1 GLCM and Remote Sensing

A comparative study conducted by Kilpelä and Heikilä (1990) reported that for remotely sensed images, the co-occurrence matrix is more efficient than other methods of texture analysis such as the Fourier spectrum and fractal dimensions. Another study conducted by Gong *et al.* (1992), which compared the GLCM, simple statistical transformation (SST), and texture spectrum techniques applied on an urban SPOT image, indicated that some features derived using GLCM and SST improved the accuracies of spectral classifications.

Many researchers have used the GLCM method with success in a variety of remote sensing applications. Conners *et al.* (1984) obtained higher classification accuracies by segmenting a high-resolution black and white image of an urban area using GLCM texture operators. Franklin and Peddle (1990) found that some features of the GLCM such as entropy and inverse difference moment derived from directional spatial co-occurrence matrices combined with spectral features improved the global classification accuracy of Spot images. Mather *et al.* (1998) concluded that of the four methods they used for texture analysis in their study on lithological discrimination using Landsat TM spectral data and textural data extracted from SAR imagery, the GLCM and the multiplicative autoregressive random field approaches performed better than the Fourier and multi-fractal based techniques. Kurosu *et al.* (2001) applied GLCM texture images and the aggregation technique for the land use classification of SAR images. Franklin *et al.* (2001) obtained results that showed that the second-order co-occurrence texture measure homogeneity out-performed the first-order texture measure variance in their texture study of IKONOS imagery for Douglas-fir forest age separability. Kiema (2002) conducted a study based on GLCM texture analysis and the fusion of Landsat TM imagery with SPOT data. Ndi Nyoungui *et al.* (2002) evaluated speckle filtering and texture analysis approaches for land cover classification using SAR images and found that the texture features that performed the best were derived from second-order and third-order GLCM.

CHAPTER 4

Classification

4.1 Digital Remote Sensing Image Data

There are three major aspects that characterize digital remote sensing image data: spatial resolution, spectral resolution and radiometric resolution. The spatial resolution of the data is the equivalent in kilometres, meters or even centimetres on the ground, of its smallest components available for processing from the original image: discrete picture elements, known as pixels, the size of which varies according to the sensor system. The radiometric resolution of an image refers to the number of binary digits, or bits, needed to represent the range of available discrete brightness levels, known as digital numbers (DN), which are the quantized radiance values recorded for each pixel by the sensor. The spectral resolution of the image data corresponds to the wavelength bands, or channels, in the electromagnetic spectrum, in which the image is acquired. This is usually a measurement of the spatial distribution of reflected, or emitted, radiation in the ultraviolet, visible and near-to-short wave infrared range of wavelengths, known as the solar spectrum. Sometimes, it can be a measurement of the spatial distribution of energy emitted by the earth itself in the thermal infrared wavelength region. It can also be a measurement of the relative backscatter from the earth's surface of energy actually emitted from the remote sensor itself in the microwave band of wavelengths (Schowengerdt, 1997; Richards and Jia, 1999; Jensen, 2000).

The concept behind multispectral remote sensing is that different materials covering the earth's surface, or their spatial properties, can be identified and assessed based on the differences in their spectral reflectance characteristics. As such, if remote sensors capture data at several wavelength bands, or channels, then identification of different land cover types should be possible. Remote sensing systems are therefore designed to gather several samples of the spectral reflectance in one or more wavelength bands. Multispectral remote sensing systems acquire image data in several spectral bands. Data recorded in a large number of spectral channels is referred to as hyperspectral data. When a single spectral band or broadband is used to capture the image it is called panchromatic data. Analysis of the spectral reflectance samples for each pixel

can be performed, through visual techniques or automated approaches, to associate the pixel with a particular land cover type (Schowengerdt, 1997; Richards and Jia, 1999; Jensen, 2000).

4.2 Image Classification: A Quantitative Analysis

The objective of image classification, as opposed to photo-interpretation, is to improve the qualitative visual analysis of image data with a quantitative analysis through automated identification of features in a remotely sensed scene. This is desired because of the fact that a computer can discriminate to the limit of the radiometric resolution available in the imagery; it can analyse at the pixel level and can examine and identify as many pixels as needed, thus taking full account of the spatial, spectral and radiometric detail present (Schowengerdt, 1997; Richards and Jia, 1999).

Automated interpretation of remote sensing images is considered a quantitative analysis due to its capacity to identify pixels based on their numerical properties and to provide area estimates by counting pixels. It is also generally called classification, which is a method by which labels are attached to pixels according to their spectral characteristics by a computer, which is trained beforehand to recognize pixels with similar spectral properties (Richards and Jia, 1999). Typically, this process involves the analysis of digital image data and the application of statistically based decision rules for determining the land cover or land use identity of each pixel in an image; the pixels are then classified into their respective ground cover classes.

In the process of multispectral classification, pixels are sorted into a finite number of individual spectral classes, known as information classes, based on the spectral pattern present within the data for each pixel. The spectral pattern is composed of the set of radiance measurements, or brightness values, obtained in the various spectral bands for each pixel. These spectral classes are what the computer works with in order to perform the quantitative analysis (Richards and Jia, 1999).

Pixels are assigned to spectral classes through a specific set of criteria, composed of the decision rules, which are developed during the training phase of the classification. These decision rules are based on the spectral radiances observed in the data; thus the process is called spectral pattern recognition, as opposed to spatial pattern recognition. These spectral classes may

be associated with known features on the ground or they may only represent areas that appear different to the computer. The intent of the classification process is to label all pixels in a digital image as belonging to one of several land cover and land use classes, otherwise known as "themes." The categorized data can subsequently be used to create a thematic map of the land cover and land use present in an image, as well as to produce summary statistics of the areas covered by each land cover or land use type (Jensen, 1996; Schowengerdt, 1997; Richards and Jia, 1999; Jensen, 2000).

4.3 Classification Methods

There are two general approaches to the classification process: supervised and unsupervised classification. Supervised classification is closely controlled by the image analyst and requires extensive knowledge of the data and of the classes desired. Unsupervised classification is more computer-automated and is dependent upon the data itself for the determination of the spectral classes; the analyst then identifies these classes after classification. This method is typically employed when there is no a priori knowledge about the data before classification, thus it offers an easy, unbiased analysis. Supervised classification introduces analyst bias, but works better than unsupervised classification when the features of interest are not clearly discriminable (Jensen, 1996; Schowengerdt, 1997; Richards and Jia, 1999).

4.3.1 Unsupervised Classification

In the unsupervised classification technique, the inherent structure of image data is determined by the computer without the need of external information. Pixels in an image are classified into spectral classes naturally present in the scene through the use of one of a variety of clustering algorithms. Clustering is the grouping of pixels in multispectral space according to their spectral similarities (Jensen, 1996).

To perform the classification, the analyst has to define areas of the image in order to train the classifier. These areas, however, do not have to be from homogeneous regions of the image. In fact, it is better to select heterogeneous regions so that all classes of interest and their within-class variabilities are taken into account. The analyst then uses a computer algorithm that locates the concentrations of spectrally similar pixels in the heterogeneous sample. These clusters are

considered to represent classes in the image and are used to derive class signatures. As a result, these methods can be used to determine the number and location of the spectral classes, as well as the spectral class each pixel belongs to (Schowengerdt, 1997).

When the clustering process is complete, pixels in each group are given a symbol to show that they belong to the same spectral class, or cluster. With these symbols, a cluster map can be created, which corresponds to the image that has been segmented. In the cluster map, the pixels are represented by their symbol, and not by the original multispectral data. The analyst can then determine the land cover identity of the spectral classes through interpretation or by associating a sample of pixels in each class with available reference data, such as maps or information from field visits. All the pixels with the same symbol can subsequently be associated with the corresponding class (Jensen, 1996; Schowengerdt, 1997; Richards and Jia, 1999).

As a result, unsupervised classifiers do not depend on training data as a basis for classification, which is advantageous when reliable training data cannot be obtained or is too expensive to acquire. Therefore, spectrally separable classes are determined before their informational value is defined. This technique is very different from, yet complementary to, the supervised approach in which useful information categories are defined before their spectral separability is examined (Jensen, 1996; Schowengerdt, 1997).

4.3.2 Supervised Classification

Supervised classification approaches are the most common techniques used to extract quantitative information from remote sensing images. In this type of classification, the analyst provides the computer algorithm with numerical descriptors of the various land cover types present in the scene, which are then used to segment the image (Jensen, 1996).

In order to accomplish this the user must determine the different land cover types, or information classes, into which the image is to be segmented. From each class, a sample of representative pixels, called training data, is selected. Two approaches for obtaining samples of training data from an image can be used. The analyst can manually delineate areas containing the prototype pixels using a reference cursor, which is controlled by a track ball, digitizer, mouse, keyboard strokes, etc. The polygons formed in this process are carefully chosen to avoid pixels

located along the edges between land cover types. These regions are usually referred to as training sites (Jensen, 1996).

The more automated seed pixel method, based on region growing algorithms, can also be employed. With this technique a single seed pixel is placed, with the display cursor, within a prospective training site that is thought to be representative of the surrounding land cover class. Subsequently, pixels with spectral characteristics similar to those of the seed pixel are selected according to various statistically based criteria. These selected pixels become the training data for that training site. This approach is useful for the delineation of irregular training sites of difficult classes such as an asphalt class that is made up of narrow roads, or a shallow water class extracted from a river. Regardless of the delineation method employed, a minimum of 10n to 100n (where n is the number of spectral bands) sample pixels will generally be needed to ensure a good statistical representation of each spectral class (Jensen, 1996; Schowengerdt, 1997).

This training stage requires substantial reference data and a thorough knowledge of the geographic area to which the data apply in order to find suitable representative areas for each class. This information can be obtained from field visits, maps, aerial photographs, or colour composites produced from the image data. If the image contains enough distinct visual cues though, the training fields may be located through visual examination. Since the goal here is to assemble a set of statistics that describes the spectral response characteristics for each land cover type to be classified in an image, the training data must be both representative and complete; it must be a homogeneous sample, yet it needs to cover the range of variability within the class. If an information class has uniform spectral response characteristics over its entire extent, a single training site should be sufficient to adequately describe this single spectral class. If, however, an information class is not uniform, which is usually the case, then a separate training area will be needed for each of the spectral classes it encompasses. Therefore, the number of training sites required to adequately represent the spectral variability in an image can sometimes be quite high (Schowengerdt, 1997; Richards and Jia, 1999).

After establishing the training sites, the data is used to create a spectral response pattern for each class based on the distribution of its spectral reflectance in each spectral band of the image. The training data also allows the estimation of the parameters of the particular classifying

algorithm to be used. These spectral patterns and parameters form the class signatures. Each individual pixel in the whole image data is then compared numerically to these signatures. According to the classifier parameters, which constitute the decision rules, the most likely class the pixel belongs to in the image is determined; the pixel is then labelled or classified accordingly (Jensen, 1996, Schowengerdt, 1997).

4.3.3 Probability Distributions

Supervised classification techniques can be divided into two categories: parametric and nonparametric. Parametric approaches are based on assumptions about the form of the probability distribution for each spectral class in multispectral space, and estimates of the distribution parameters. Nonparametric algorithms are not based on such statistical distribution models or their parameters, but rather on the spectral distance between classes (Schowengerdt, 1997).

A probability distribution is multidimensional, with as many variables as there are dimensions of the space. It describes the likelihood of finding a pixel belonging to a certain class at any given location in multispectral space. This is possible since a multivariable distribution is designated by the way that most pixels in a distinct cluster or spectral class lie near the centre and decrease in density away from the centre. The most common distribution model used for applications in multispectral remote sensing is the multivariate normal, or Gaussian, distribution. This is due to the fact that it provides tractable mathematical solutions for the analysis of decision boundaries in the supervised classification process, and because the image samples used for supervised training usually present normal distributions; even if certain distributions are not normal, the classification accuracy will not be overly affected (Schowengerdt, 1997; Richards and Jia, 1999).

The Gaussian probability distribution is characterized by its two parameters: the mean vector, which describes the mean position of the spectral class, and the covariance matrix, which describes the directional distribution of the class in multispectral space. As a result, spectral classes that are modelled by the normal distribution are also described by these two parameters. Therefore, if these two parameters can be calculated for each class, then the set of probabilities that present the likelihoods of finding a pixel at a particular location belonging to each of those

classes can also be calculated. The class that indicates the highest probability can then be considered the class to which the pixel belongs. Thus if the mean position and the covariance matrix for every spectral class in an image can be calculated, then based on the probabilities of the specific location of a pixel, every pixel in the image can be examined and labelled according to the class it most likely belongs to. In the supervised classification, these two parameters are estimated for each class from the pixels representing the training samples (Jensen, 1996; Schowengerdt, 1997).

4.4 Classification Approaches in Remote Sensing

A number of different supervised and unsupervised strategies have been used in remote sensing image classification. Unsupervised classification approaches are usually based on clustering algorithms such as the migrating means, single pass, agglomerative hierarchical, and histogram peak selection clustering techniques. These methods generally employ some process to measure the similarity between pixels that belong to a particular cluster, called similarity metrics, which are usually simple distance measures. These distance measures are then used to determine clusters in the data (Jensen, 1996; Richards and Jia, 1999).

The supervised classification is the method most often used for the quantitative analysis of remote sensing image data. It is based upon the use of suitable algorithms to label the pixels in an image as representing particular ground cover types, or classes (Richards and Jia, 1999). The method of supervised classification requires a priori knowledge of the objects of interest in order to create training sites, which are then used to "train" the system in order to generate the spectral signatures for these classes. The system thereafter labels all pixels belonging to each particular class according to a decision rule.

Supervised classifications consist of numerous different methods; each strategy has its associated strengths and weaknesses. Among nonparametric classifiers, the level-slice approach, also known as the box classifier, is a simple, as well as computationally efficient technique, which is based on the extraction of upper and lower spectral bounds, through analysis of histograms of each spectral component of a class, used to indicate the edges of a multi-dimensional box. Pixels within the box are labelled according to that class. It is, however, not a very appropriate classifier for remote sensing data since pixels that are found outside of the box

will not be classified, and pixels that are found in the overlapping regions of the boxes will be inseparable. A modification of this method, the parallelepiped classifier, is also quite fast and computationally efficient as well as being sensitive to category variance, although it is insensitive to covariance. The histogram estimation technique is a fast classifier, but it does not account for spectral vectors for every class. The nearest-neighbours classification methods assign labels to unknown pixels based on the labels of the neighbouring training pixels; it is however, a computationally slow technique. The Mahalanobis classifier is very much like a minimum distance classifier, but its distance measure is sensitive to direction and can be modified according to class. A more recent nonparametric classification strategy is the artificial neural network classifier (ANN). This approach is similar to clustering algorithms. Training of the ANN is accomplished through the back-propagation algorithm (Jensen, 1996; Schowengerdt, 1997; Richards and Jia, 1999).

Among the parametric classification methods, the minimum-distance-to-mean classifier is based on the mean positions of the spectral classes, making it a useful technique in cases of limited training samples. It is mathematically simple and computationally efficient, but it is insensitive to different degrees of variance in the spectral response data. Because of this, it is not typically used when spectral classes are close to one another and have high variance. The maximum likelihood classifier (MLC), otherwise known as the Bayes classifier, evaluates both the variance and covariance of a spectral class when classifying an unknown pixel. If the underlying probability distributions can be correctly estimated, then this approach can minimize the total classification error. The principle drawback of this technique is the large number of computations required to classify each pixel (Schowengerdt, 1997; Richards and Jia, 1999).

4.5 Maximum Likelihood Classification

The maximum likelihood classification (MLC) technique is the most popular and widely used among all supervised classification methods (Mather *et al.*, 1998); it calculates the greatest probability that a pixel belongs to a given class, thus minimizing pixel misclassifications.

The MLC usually assumes multivariate normal models. This normal distribution is defined as a function of a vector location in multispectral space by:

$$p(\boldsymbol{x}) = 1 / [(2\pi)^{N/2} |\Sigma|^{1/2}] \exp\{- \tfrac{1}{2} (\boldsymbol{x}- \boldsymbol{m})^t \Sigma^{-1} (\boldsymbol{x}- \boldsymbol{m})\} \quad (2.1)$$

where $\boldsymbol{x}$ is a vector location in the N dimensional pixel space, $\boldsymbol{m}$ is the mean position of the spectral class, and Σ is the covariance matrix of the distribution. The MLC is originally based on the Bayes' classification. In its final form, the MLC for normal distributions is:

$$g_i(\boldsymbol{x}) = \ln p(\omega_i) - \tfrac{1}{2} \ln |\Sigma_i| - \tfrac{1}{2} (\boldsymbol{x}-\boldsymbol{m}_i)^t \Sigma_i^{-1} (\boldsymbol{x}-\boldsymbol{m}_i) \quad (2.2)$$

where $g_i(\boldsymbol{x})$ is the discriminant function, ω_i is the spectral class of an image, $p(\omega_i)$ is the probability that class ω_i occurs in the image, $\boldsymbol{m}_i$ is the mean vector and Σ_i is the covariance matrix of ω_i.

ω_i is represented by: $\omega_i, i = 1, \ldots M$

where M is the total number of classes.

4.5.1 MLC and Remote Sensing

A variety of remote sensing applications have seen the successful employment of the maximum likelihood classifier. Using airborne multispectral images, Franklin *et al.* (2000) incorporated texture into MLC classification of forest species composition. In a case study on the monitoring, classification and evaluation of the urbanization process in Africa, Balzerek (2001) applied the MLC on high spatial resolution IKONOS satellite scenes. Kurosu *et al.* (2001) conducted a study on land use classification with textural analysis on SAR images in which they employed the MLC approach. Shaban and Dikshit (2001) evaluated the MLC and GLCM texture features for the urban classification of SPOT imagery. Kiema (2002) used the MLC and texture analysis to extract topographic objects from fused Landsat TM and SPOT images.

CHAPTER 5

Description of Study Area and Image Data

5.1 Study Area

The study site for this research project covers the principal section of the old city of Sherbrooke, which represents the core of urbanization for the area commonly known as "Estrie". Two major rivers flow through this region: the Magog River runs in a generally northeast direction through the site, towards the middle of the city where it meets the Saint François River, which flows in the general direction of northwest from the southeast. The narrow gorge of the Magog River surges over a short distance in the heart of downtown Sherbrooke. In the southwestern region of the study area, Mount Bellevue, a natural recreational site, sits on the outskirts of the city, not far from the Magog River. The University of Sherbrooke grounds are located just west of Mount Bellevue.

The area of interest for this study consists of various types of land use, such as road network, agricultural, residential, commercial, industrial, institutional, and recreational uses. Different land cover types that compose the region are river, bare soil, grass, shrubs and forest. As such, this site provides a good study area for the purposes of urban land use and land cover classification analysis.

The old city of Sherbrooke is located in the Eastern Townships of the southern region of the province of Quebec, Canada. It is located between 45°18' and 45°27' latitude north, and 71°48' and 72°02' longitude west. The study site of Old Sherbrooke covers an area of approximately 11 km x 11 km. The topography of the site is generally hilly, with heights ranging from about 200 meters to 400 meters above mean sea level. The region is abundantly vegetated with grass and trees, especially towards the outer edges of the city where there are large sections of dense coniferous and deciduous forests mixed with shrubs and grassy fields, and patches of agricultural land. Within the city, considerable expanses of forest and grassland, concentrated along the two rivers, compose various recreational areas.

Geographical Location of Study Area:
Sherbrooke, Québec, Canada

UTM Projection: **Northern Hemisphere** **Zone 18** **NAD83**

Author: Shahid Kabir Université de Sherbrooke Winter 2002

Figure 2: Geographical Location of Study Area

5.2 Research Data

High spatial resolution images obtained by the IKONOS-2 satellite of Space Imaging were selected for this research project. The 16-bit raw multispectral and panchromatic satellite scenes of the Old Sherbrooke area were acquired on May 20, 2001 at 10:50 am, local time. The scenes have an image dimension of approximately 11800 x 13200 pixels, and were standard geometrically corrected at the source. The map projection used is Universal Transverse Mercator; the UTM specific parameters are: Northern Hemisphere, zone 18, North American Datum (NAD) 83.

Bands	**Resolutions**	
Multispectral	Spectral Properties	Spatial Properties
Red	0.63-0.69 µm	4 x 4 meters
Green	0.52-0.60 µm	4 x 4 meters
Blue	0.45-0.52 µm	4 x 4 meters
Near Infrared	0.76-0.90 µm	4 x 4 meters
Panchromatic	0.45-0.90 µm	1 x 1 meter

Table 1: Data Description

Supplementary data was used in this study for the creation of training and verification sites, as well as for the verification of the classifications. These data were obtained from the following sources: NTDB (National Topographic Data Bank) of the Sherbrooke region, having a scale of 1:50 000, that was produced in 2000 by the Centre for Topographic Information department of Natural Resources Canada, black and white aerial photographs of the area taken in September 1998 and August 2000, at a scale of 1:15 000 and 1:40 000 respectively, obtained from the Photocartothèque Québécoise of the Ministry of Natural Resources Québec, and in-situ data

collected during field visits. Also used, was a topographic map of the Sherbrooke area from Canadian Topographic Maps. The map has a scale of 1:50 000, and was produced in 2000 by the Centre for Topographic Information division of Natural Resources Canada.

CHAPTER 6

Methodology

6.1 Introduction

In order to fulfill the objectives of this study, a methodology was developed based on the two major elements of this research: texture analysis and spectral-spatial classification. These two processes were employed for the extraction of spatial information, as well as for the creation of an urban land cover and land use classification map, from the high spatial resolution IKONOS images.

In the texture analysis phase of the methodology, the grey level co-occurrence matrix (GLCM) technique was used, which consists of five main stages for the creation of the texture images to be integrated in the classification process: delimitation of the study site, selection of the distance between pixels, selection of the direction between pixels, selection of the appropriate window size, and finally, selection of the most useful texture features.

The classification phase of the methodology involves the following six steps based on the maximum likelihood classification (MLC) method, which resulted in the production of a thematic map of the Old Sherbrooke study site: integration of spectral and spatial data for classification, creation of training and verification sites, verification of class separability, creation of pseudo-colour table, post classification filtering, and lastly, estimation of classification precisions.

These steps, which can be visualized from the methodology flow chart presented in Figure 3, are further elaborated for the two techniques throughout the rest of this chapter.

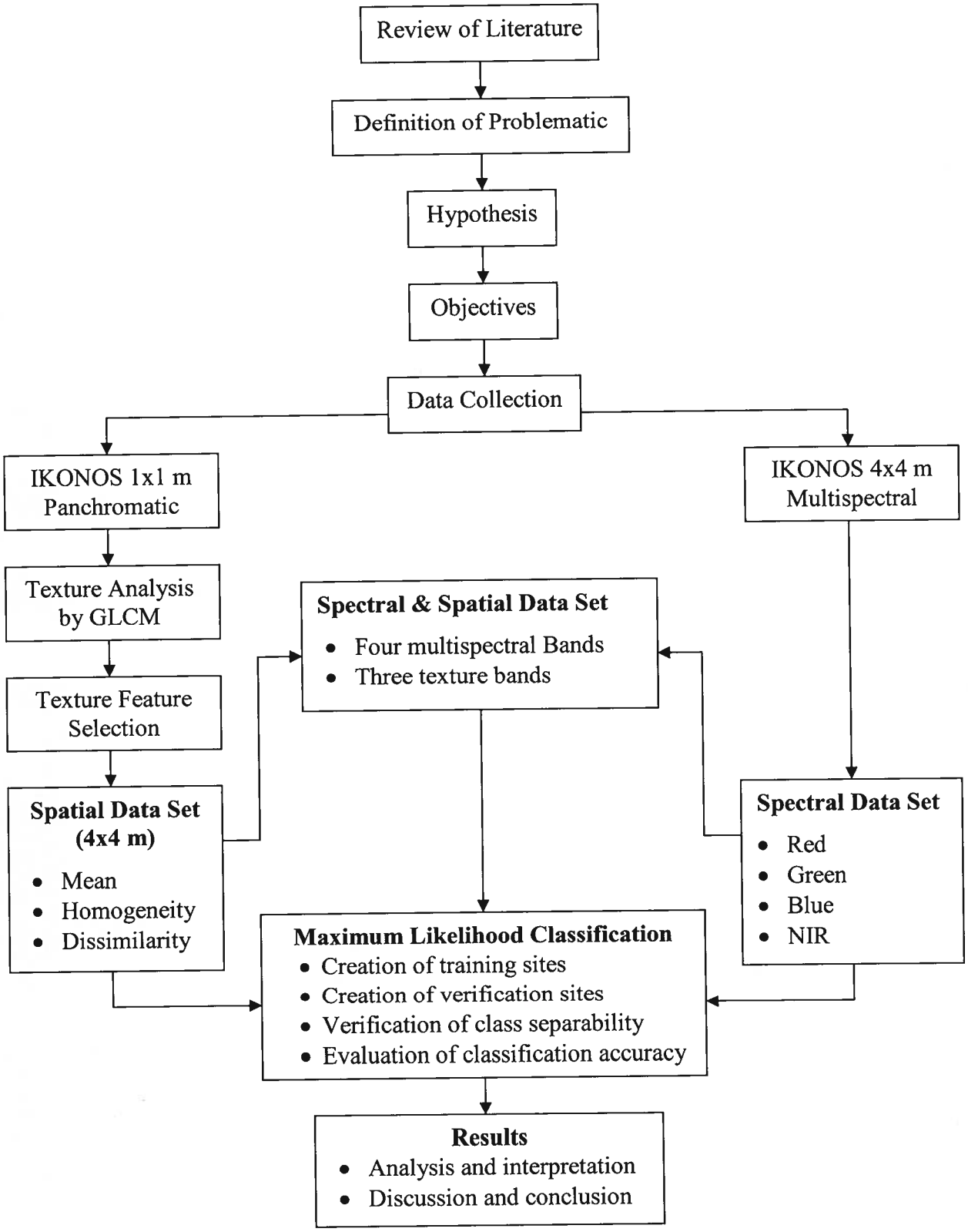

Figure 3: Methodology Flow Chart

6.2 Delimitation of Study Site

The raw panchromatic and multispectral IKONOS scenes of the Old Sherbrooke area were cropped in order to reduce the image matrix to 11000 x 11000 pixels. This delimitation of the study site resulted in a better representation of the objects of interest (See Figure 4).

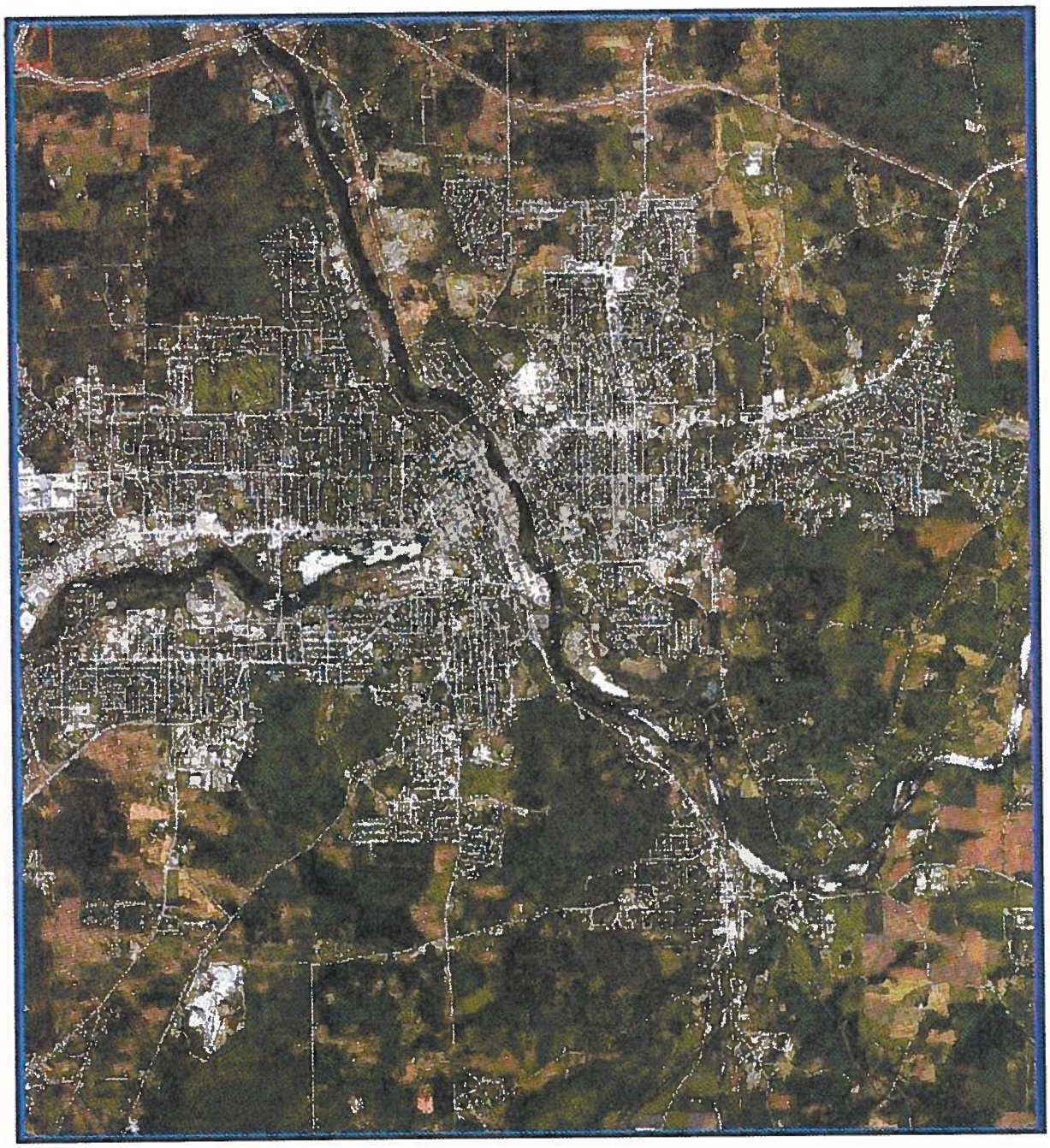

Figure 4: RGB Colour Composite of the Old Sherbrooke Study Site

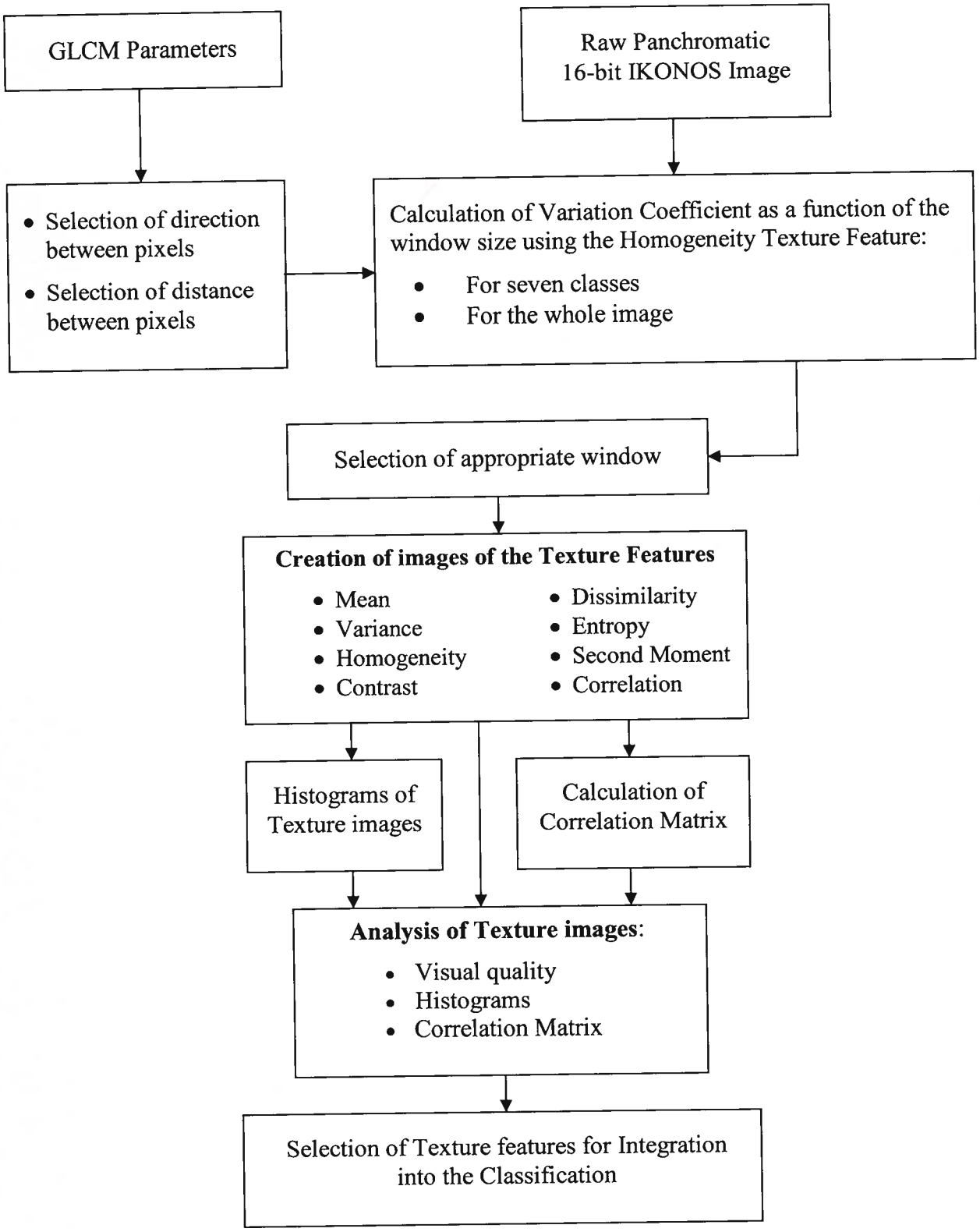

Figure 5: GLCM Texture Analysis Flow Chart

6.3 Grey Level Co-occurrence Matrix Parameters

In this study, the Grey Level Co-occurrence Matrix (Haralick *et al.*, 1973) was used as the method of extracting textural information from the panchromatic IKONOS satellite scene (See Figure 5). The success of the GLCM method of texture analysis is directly related to the appropriate choice concerning three parameters: the distance between pixels, the direction between pixels, and the size of the window to be used. The results of classifications performed using textural data are greatly influenced by these variables; therefore, many processes have been developed to facilitate the determination of suitable selections for these factors.

6.3.1 Selection of Distance Between Pixels

In an urban scene, there exist numerous textures with greatly varying degrees of smoothness or coarseness. The choice of the appropriate distance depends on the smoothness or coarseness of the texture of interest. Therefore, to choose the most suitable distance between pixels is not easy. However, it has been found that small distances produce the best results (Karathanassi *et al.*, 2000; Weszka *et al.*, 1976), since they are appropriate for textures that are fine, as well as for those that are coarse. As a result, a distance equal to 1 pixel, which is also the most commonly used, was chosen for this study.

6.3.2 Selection of Direction Between Pixels

For the direction between pixels, one method that can be used consists of calculating the features of the co-occurrence matrix for the four directions of 0°, 45°, 90° and 135°, and to take their averages (Haralick, 1979). Another study has shown that certain directions can provide a better discrimination between classes than the method of taking the average of all the directions (Franklin and Peddle, 1989). However, the most common choice for the direction between pixels found in literature is 0°, which is what was used in this study by default of the image processing system used.

6.3.3 Selection of Appropriate Window Size

The accuracy of the classification process using texture features depends on the size of the window used. If the window is too small, enough spatial information will not be extracted in order to characterize a certain type of land cover. On the other hand, if the window is too large, it

will either overlap onto two types of land cover and introduce the wrong spatial information (Pultz and Brown, 1987), or it will create transition limits that are too large between two types of neighbouring land cover (Gong, 1990). If the window size is too small or too large relative to the texture structure, then texture features will not accurately reflect real textural properties (Mather *et al.*, 1998).

In order to choose an appropriate size for the window, a method can be used that is based on the calculation of the variation coefficient for each class as a function of the size of the window, using a given texture feature (Laur, 1989). The appropriate window size will be that for which the variation coefficients start to stabilize for the majority of the classes, while having the lowest value.

In this study, the homogeneity texture feature was randomly chosen for the calculation of the variation coefficients for each class according to different window sizes. The variation coefficients started to stabilize at the 11x11 pixel window for the majority of the classes (See Figure 6).

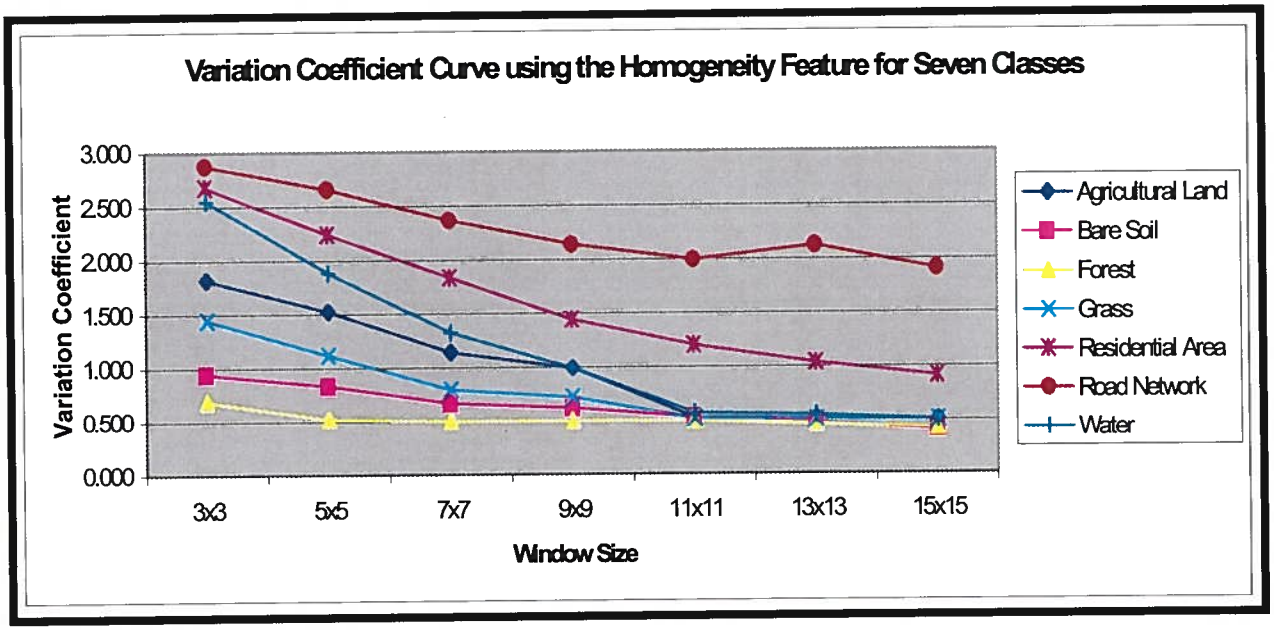

Figure 6: Variation Coefficient Curve using the Homogeneity Feature for Seven Classes

As a result, the 11x11 window was chosen for use in the calculation of the texture features for the purposes of this study.

6.3.4 Selection of Texture Features

There are as many as fourteen different texture features that may be extracted from co-occurrence matrices (Haralick *et al.*, 1973; Haralick, 1979). The image processing system used in this study only allows the use of the following eight texture features: Contrast, Correlation, Dissimilarity, Entropy, Homogeneity, Mean, Second Moment, and Variance. Many of these features are redundant and capture similar concepts (Wilson, 1996). Thus, the following process was employed in order to eliminate the superfluous texture features and to choose the most useful features for good urban class discrimination.

From the panchromatic image, texture neo-channels of the eight different features were produced using the 11x11 pixel mobile window that was determined to be the most appropriate window size, with the direction of 0° between pixels, and with the distance of 1 pixel between pixels.

For the first step in the process of elimination, the visual quality of these texture images was analysed and three features, Correlation, Entropy, and Second Moment, were initially considered for discarding due to their poor quality in terms of visual information (See Figure 7).

After displaying the histograms of all the channels, it was confirmed that these three features, Correlation, Entropy, and Second Moment were to be eliminated due to the small and narrow peaks they presented. The possible elimination of another two features, Contrast and Variance, was also considered from the histogram analysis because of the same reason (See Figure 8).

Finally, through calculation of the correlation matrix, it was confirmed that these two features, Contrast and Variance, as well as the first three features, Correlation, Entropy, and Second Moment, were to be discarded due to their relatively high correlation with the other features (See Table 1). As a result, only three texture features, Mean, Homogeneity, and Dissimilarity, were selected for use in this study.

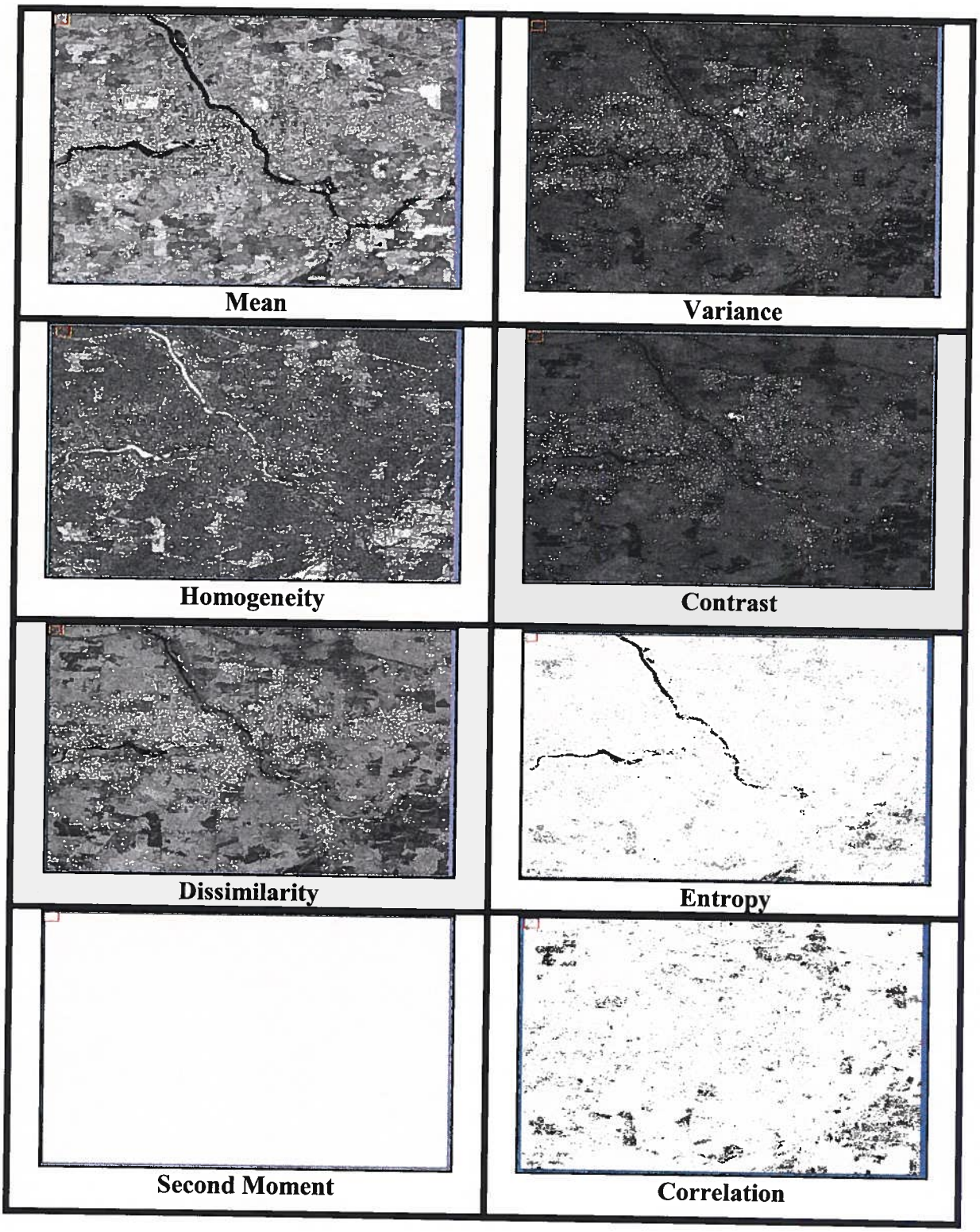

Figure 7: Neo-Channels of the Eight GLCM Texture Features

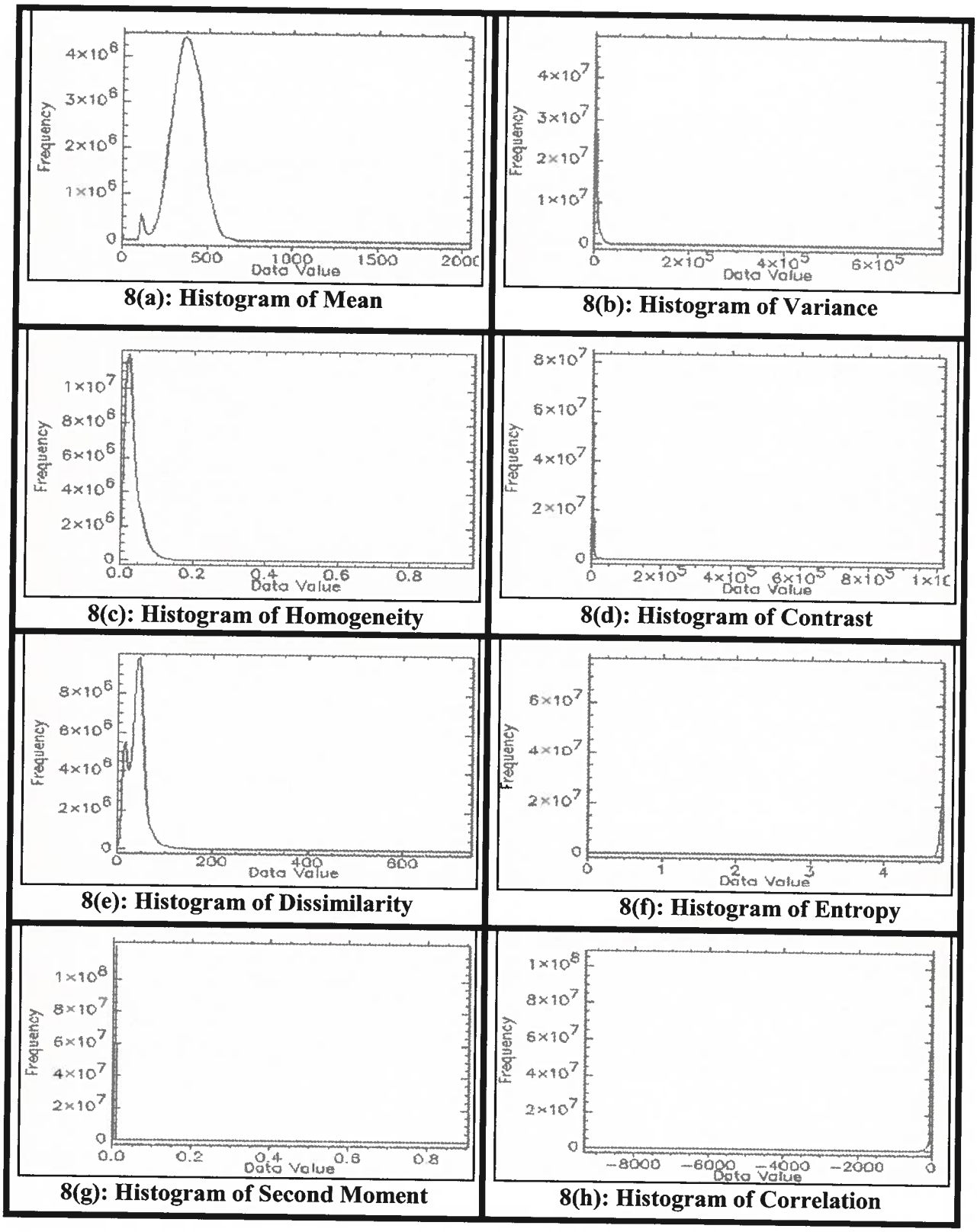

Figure 8: Histograms of the Eight Texture Bands

Band	Mean	Variance	Hom	Contrast	Dis	Entropy	SM	Cor
Mean	1	0.219588	-0.01689	0.202036	0.105681	0.207555	0.002025	-0.236810
Variance	0.219588	1	-0.14096	0.828535	0.68651	0.028310	0.008660	0.113488
Homogeneity	-0.01689	-0.14096	1	-0.15298	-0.52143	-0.095520	0.407330	-0.347840
Contrast	0.202036	0.828535	-0.15298	1	0.775256	0.028838	-0.000300	0.104926
Dissimilarity	0.105681	0.68651	-0.52143	0.775256	1	0.133169	-0.062690	0.337697
Entropy	0.207555	0.02831	-0.09552	0.028838	0.133169	1	-0.007470	0.001700
Second Moment	0.002025	0.00866	0.40733	-0.0003	-0.06269	-0.00747	1	-0.014240
Correlation	-0.23681	0.113488	-0.34784	0.104926	0.337697	0.00170	-0.014240	1

Table 2: Calculation of the Correlation Matrix

6.4 Classification through Maximum Likelihood

For the purposes of this study, the maximum likelihood classification approach was used to extract the urban data from the high spatial resolution IKONOS imagery (See Figure 9). This supervised classification method was used because of its popularity, and due to the proximity and familiarity of the Sherbrooke area, as well as the easy accessibility of field data.

6.4.1 Integration of Spectral and Textural Data for Classification

Many researchers have developed different methods of integrating textural data with spectral data (Tso, 1997; Franklin *et al.*, 2000; Kurosu *et al.*, 2001). However, the most widely used method is that of using the textural data as neo-channels to be combined with the spectral channels in the classification process (Marceau *et al.*, 1990; Coulombe *et al.*, 1991; Mather *et al.*, 1998; Shaban and Dikshit, 2001).

In this study, the input images were: the four multispectral images (Red, Green, Blue and Near Infrared), and the three textural images (Mean, Homogeneity, and Dissimilarity), which were produced from the steps in the textural analysis process. These images were integrated in the classification procedure.

For the purposes of comparison, three input datasets were created for classification:

- A spectral dataset consisting of the Red, Green, Blue and N-IR bands.
- A spatial dataset consisting of the Mean, Homogeneity and Dissimilarity texture bands.
- A combination dataset consisting of the spatial and spectral datasets.

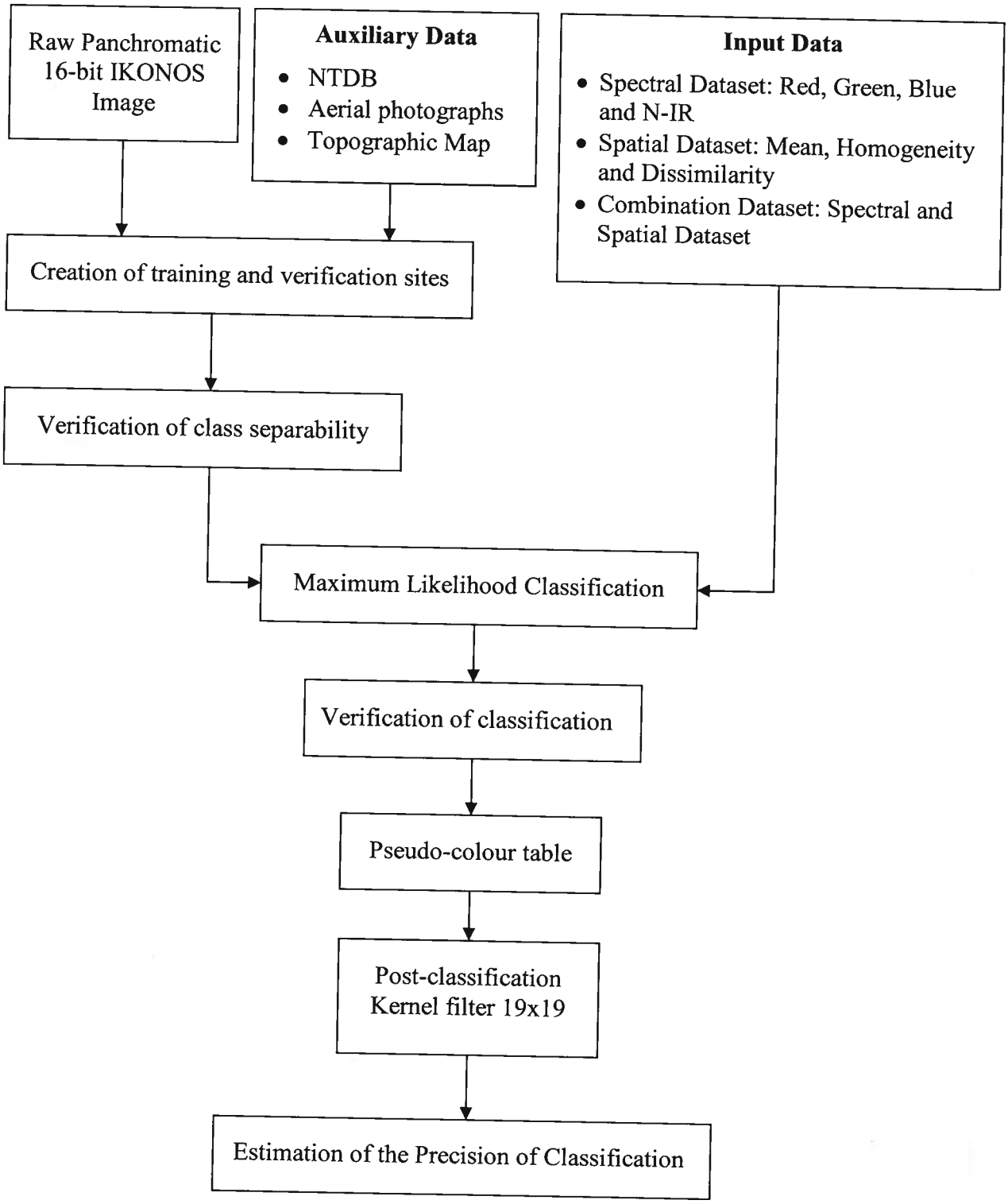

Figure 9: Maximum Likelihood Classification Flow Chart

6.4.2 Creation of Training and Verification Sites

Since the maximum likelihood classifier used for the supervised classification technique employed in this study requires a good amount of knowledge about the object characteristics of the Sherbrooke area, this information was obtained through field visits, topographic maps, aerial photographs and NTDB layers of Sherbrooke.

Training sites were selected from several spectrally distinct classes for the generation of information classes (Kershaw and Fuller, 1992). These training samples were used to "train" the classifier to recognize the different spectral classes in the image so that each pixel could subsequently be compared to them in the labelling phase. The verification sites were created for each class from areas on the image where the training sites were not produced.

In order to avoid poor classifications or inaccurate estimates of the elements, efforts were made to choose a sufficient number of training pixels for each class. The classes used for this study were selected after careful determination of their adequate representation of the whole image. Training and verification sites for the following twelve land use and land cover classes were created for this study:

- Agriculture
- Asphalt and Parking Lot
- Bare Soil
- Commercial Area
- Coniferous Forest
- Deep Water
- Deciduous Forest
- Grass
- Residential Area
- Road Networks
- Shallow Water
- Shrubs

Classes	Training Sites		Verification Sites	
	Numbers of pixels	Number of Segments	Numbers of pixels	Number of Segments
Agricultural	1777437	61	126048	35
Asphalt and Parking Lot	29747	37	29101	41
Bare Soil	1022180	32	344993	11
Commercial, Industrial & Institutional	138933	23	43411	29
Coniferous Forest	110478	17	87200	14
Deciduous Forest	396508	12	290914	9
Deep Water	24620	27	27063	30
Grass	756013	68	148856	21
Residential Area	12130	69	7573	54
Road Networks	7692	44	25192	27
Shallow Water	16453	18	12985	17
Shrubs	46227	32	20570	29

Table 3: Training and Verification Sites

6.4.3 Verification of Class Separability

In the classification process, the spectral classes produced by the training sites must be sufficiently separate in order for the classifier to differentiate between the various class signatures. If the class separabilities are too low, then this will lead to a high number of misclassified pixels. As a result, it is useful to calculate the separability of the spectral classes before generating the final spectral signatures. This will allow for the improvement of low separabilities through the creation of better training sites.

The class separabilities for the training and verification sites were calculated using the Jeffries-Matusita and Transformed Divergence separability measures. These values range from 0 to 2.0 and indicate how well the selected sites are statistically separate. Although a good separability between the classes is between 1.9 and 2.0, values above 1.5 are considered acceptable by some researchers (Anys, 1995). In order to obtain a considerable separability,

many attempts were made to create sites that produced good values for class separability in this study (See Table 7).

6.4.4 Use of Pseudo-colour Table

The results of the classification can be presented in two forms: a table that summarizes the number of pixels in the whole image that belongs to each class, or a classified image. The classified image is a thematic map showing the spatial distribution of the land cover and land use present in the region of interest, in which each pixel is assigned a symbol or colour that relates it to a specific class on the ground. Thematic maps are often represented according to a pseudo-colour table, which provides for a better visualization of the classified data.

In this study, the pseudo-colour table used to represent each land cover and land use type in the final classified image of the combined datasets can be found in Figure 10.

6.4.5 Post-Classification Filtering of Classified Image

To smooth out the classified images, a Majority Analysis was applied. The Majority Analysis is used to change spurious pixels within a large single class to that class by selecting a kernel size; the centre pixel in the kernel will be replaced with the class value that the majority of the pixels in the kernel has.

Since larger kernel sizes produce more smoothing of the classified image, several attempts were made with different kernel sizes, such as 7x7, 9x9, 11x11, etc. The 19x19 kernel size displayed the smoothest appearance and was thus chosen for this study.

The centre pixel weight is the weight used to determine how many times the class of the centre pixel is counted when determining which class is in the majority; in this study a centre pixel weight of 5 was used, as it produced the best results.

6.4.6 Estimation of Classification Precision

The final step of the classification is the evaluation of the precision of the results obtained. This will indicate how well the classification performed and whether or not the objectives have been achieved. Once the spectral space is segmented into different regions

associated with classes of objects, each pixel of the verification sites is assigned the label of the class that represents it in the segmented spectral space. The overall result of this process is presented in the form of a confusion matrix. From this matrix many classification precision indexes can be calculated. From a comparative study done on the different methods of evaluating the classification accuracy, it was found that the most appropriate index to provide an exact classification precision is the Kappa coefficient, because it takes account of all the elements of the confusion matrix (Fung and Ledrew, 1988). This is the method that was adopted in this study.

Kappa Coefficient

$$\kappa = \frac{N\sum_{k} x_{kk} - \sum_{k} x_{k\Sigma} x_{\Sigma k}}{N^2 - \sum_{k} x_{k\Sigma} x_{\Sigma k}} \qquad (3.1)$$

where Σ is the sum over all rows in the matrix, x_{kk} is the total of marginal rows, x_k is the total of marginal columns, and N is the number of observations.

Chapter 7

Results and Analysis

7.1 Texture Analysis Results

From the texture analysis phase, the experiment conducted for determining the window size produced results that show the window size of 11x11 pixels as the most appropriate for capturing the underlying texture in the image for this particular study site. More than 65 % of the region is composed of vast forest, agricultural and grassy areas (See table 5). As a result, a large window is needed in order to extract enough spatial information to accurately reflect the textural properties of these classes.

During the selection of the texture features, analysis of the visual quality of the texture images revealed that out of the eight features considered, the Second Moment feature is completely devoid of any information. The Correlation and Entropy features provide some information, but not enough for adequate discrimination. The texture images of Variance and Contrast are similar in nature, which indicates redundancy in one of the two. Although they both present more information than Correlation and Entropy, they do not allow for sufficient texture distinction. The Mean, Homogeneity and Dissimilarity texture features all provide unique textural details that are easily discernable in the images (See Figure 7).

The histogram analysis of the texture features produced much the same outcome. The Second Moment, Variance Contrast, Entropy and Correlation histograms have very little or no peaks, indicating a lack of texture information and discrimination power. The Mean, Homogeneity and Dissimilarity histograms presented distinct peaks, which is consistent with the quality of their texture images (See Figure 8).

7.2 Classification Results

The following two tables present the results of the classification process. Table 4 shows the classification accuracies obtained for each class resulting from the classifications conducted on each of the three datasets, as well as the overall accuracies and Kappa coefficients produced for each dataset. Table 5 is the statistical representation of the final classification done with the

combination of spectral and spatial data. These final classification results are also presented in the form of a thematic map in Figure 10.

	Spectral Data (Red, Green, Blue and NIR)	Spatial Data (Mean, Homogeneity and Dissimilarity)	Combination Data (Spectral and Spatial)
Kappa Coefficient	0.74	0.68	0.83
Overall Accuracy (%)	78.9	73.5	86.1
Classes	**Classification Accuracies (%)**		
Agriculture Land	73.9	70.6	88.9
Asphalt and Parking Lot	64.3	61.2	86.5
Bare Soil	74.2	73.9	84.3
Commercial, Industrial, Institutional	68.5	59.8	83.1
Coniferous Forest	62.4	61.1	70.6
Deciduous Forest	73.9	67.8	82.7
Deep Water	87.5	84.9	90.9
Grass	77.3	72.5	89.0
Residential Area	65.8	61.4	82.8
Road Network	68.2	62.6	82.1
Shallow Water	74.7	70.7	80.9
Shrubs	62.4	61.8	71.9

Table 4: Comparative Accuracies of the Different Dataset Classifications

	Agricultural	88.9		Deep Water	90.9
	Asphalt and Parking Lot	86.5		Grass	89.0
	Bare Soil	84.3		Residential Area	82.8
	Commercial, Industrial, Institutional	83.1		Road Network	82.1
	Coniferous Forest	70.6		Shallow Water	80.9
	Deciduous Forest	82.7		Shrubs	71.9

Overall Accuracy: 86.1%

Kappa Coefficient: 0.83

Figure 10: Classification of Combined Spectral Bands and Spatial Bands

Classes	Number of Pixels in Whole Image	Percentage (%) of Whole Image
Agricultural Land	12 292 332	10.16
Bare Soil	2 193 414	1.81
Commercial	8 756 036	7.24
Coniferous Forest	9 055 436	7.48
Deciduous Forest	36 916 561	30.51
Deep Water	675 924	0.56
Grass	4 315 099	3.57
Parking Lot	2 633 992	2.18
Residential Area	15 340 348	12.68
Road Network	9 581 520	7.92
Shallow Water	1 136 101	0.94
Shrubs	18 103 237	14.96
Total	**121 000 000**	**100.00**

Table 5: Tabular Representation of the Final Combined Dataset Classification

7.2.1 Spatial Dataset

The results obtained from the classification stage of this research study show that the classification done with the purely spatial dataset (Mean, Homogeneity and Dissimilarity texture bands) produced limited accuracies ranging from 59.8 % to 84.9 % for all classes, with an overall accuracy of 73.5 %. The best accuracies obtained for this dataset are for the Deep Water, Bare Soil, and Grass classes, which have 84.9 %, 73.9 % and 72.5 % accuracies respectively.

The Commercial, Industrial and Institutional class has the lowest classification accuracy of only 59.8 %. Other classes that produced low accuracies are the Coniferous Forest, Asphalt and Parking Lot, Residential, and Shrubs classes, with 61.1 %, 61.2 %, 61.4 % and 61.8 % accuracies respectively.

7.2.2 Spectral Dataset

The classification of the purely spectral dataset (Red, Green, Blue and N-IR bands) produced somewhat higher accuracies for all of the classes compared to the spatial dataset. Here,

the accuracies range from 62.4 % to 87.5 % for all classes, with an overall accuracy of 78.9 %. This means an increase in accuracy ranging from 0.3 % to 6.1 % for each class and an overall increase of 5.4 %. The highest classification accuracies achieved with this dataset was for the Deep Water (87.5 %), and Grass (77.3 %) classes, which saw improvements of 2.6 % and 4.8 %, respectively.

The Asphalt and Parking Lot (64.3 %), Coniferous Forest (62.4 %), and Shrubs (62.4 %) classes once again produced the lowest accuracies, with an increase in classification accuracy over the textural classification of 3.1 %, 1.3 %, and 0.6 % respectively.

7.2.3 Combination Dataset

The highest accuracies obtained in this study was with the classification of the combination of the spectral and spatial datasets, which produced accuracies ranging from 70.6 % to 90.9 % for all classes and an overall accuracy of 86.1 %. The increase in classification accuracies with this dataset over the spectral dataset ranges from 3.4 % to 22.2 % for each class with an overall increase of 7.2 %. For this dataset also, the Deep Water and Grass classes once more have the highest classification accuracies at 90.9 % and 89.0 % respectively. The classes that saw the greatest increase in classification accuracy with the combination dataset is the Asphalt and Parking Lot class, followed by the Commercial, Industrial and Institutional class, the accuracies of which increased by 22.2 % and 14.6 % respectively.

The classes that obtained the lowest classification accuracies for this dataset are again the Coniferous Forest and the Shrubs classes at 70.6 % and 71.9 % respectively. The addition of textural information to the spectral data for this classification resulted in an increase in the classification accuracies of 8.2 % and 9.5 % for these two classes respectively. A statistical Z-test can be done in order to determine whether the results obtained for the different classifications are statistically different.

7.3 Interpretation of Results

The Deep Water, Bare Soil, and Grass classes obtained the highest accuracies in the spatial classification. These accuracies are acceptable when using only one panchromatic band. The lowest accuracies in the spatial classification were obtained by the Commercial, Industrial

and Institutional class, Asphalt and Parking Lot, Residential, Coniferous Forest, and Shrubs classes. The textural heterogeneity of the Commercial, Industrial and Institutional class can be explained by the irregular structures of the buildings, as well as the presence of more than one building intermingled with parking areas, such as the case of colleges and universities. The Asphalt and Parking Lot class presents heterogeneous textures possibly because of the presence of cars, which, especially in the case of parking lots, do not always have an even distribution. For the Residential class, the random mixture of roofs and treetops are likely the cause of the varying textures. As for the heterogeneity of the textures described by the Coniferous Forest and Shrubs classes, this may be due to the fact that these two classes, as well as the Deciduous Forest class, do not occupy distinct areas of the image; most of the forests in the images are a composite of these three classes. The low classification accuracies of all these classes indicate that they need the input of spectral information for greater discrimination.

In the spectral classification, the classes that produced the highest accuracies are again the Deep Water and Grass classes, which means that with either spatial or spectral information, these classes are highly discriminable. The classes that produced the lowest accuracies are the Asphalt and Parking Lot, Coniferous Forest, and Shrubs classes. This means that these classes are not easily distinguishable from other spectrally similar classes. The inability to produce representative spectral signatures for these classes may be due to various reasons. In the case of the Asphalt and Parking Lot class, this is most likely due to the presence of vehicles, which produce spurious diffuse and specular reflections that degrade the spectral signature of the pixels in this class. The fact that the forests in the image are generally mixed is probably the reason that the Coniferous Forest and Shrubs classes failed to produce representative spectral signatures. Since these classes also produced low accuracies with the spatial dataset, this means that they are not distinguishable with only spectral or textural data alone.

The Asphalt and Parking Lot class as well as the Commercial, Industrial and Institutional class showed the most increase in classification accuracy with the combination dataset. Other classes that also produced comparably high increases in accuracy are the Residential and Road Network classes. This is the expected performance of the input of textural data in the multispectral classification, since these classes obtained relatively poor accuracies with the spectral and textural datasets alone.

The lowest increases in classification accuracy with the combined data were obtained by the classes that produced relatively high accuracies with the purely spectral and textural datasets. The Deep Water class saw an increase in accuracy of only 3.4 % and the Shallow Water class only 6.2 %. Since these classes are spatially and spectrally distinguishable anyhow, the addition of texture did not make much of a contribution. This indicates that the combination of textural and spectral information is needed for those classes that produce low accuracies with purely spectral or textural data.

The lowest classification accuracies produced for the combination dataset was for the Coniferous Forest and Shrubs classes. These relatively low accuracies are reflected in the low percentages covered by these two classes in the image, where the Coniferous Forest class comprises only 7.48 % and the Shrubs class 14.96 % (See Table 5). The Deciduous Forest class, on the other hand, is shown to occupy more than 30 % of the whole image. Visual analysis of the images reveals that the Coniferous Forest class should actually make up almost half of the total of the two Forest classes. This implies that many pixels belonging to the Coniferous Forest class were probably misclassified as Deciduous Forest.

The overall classification results, however, seem very promising. Classified images of selected individual classes were generated in an attempt to evaluate the performance of the classification on a visual level. A classified image of only the Residential class is presented in Figure 11. For the Deciduous Forest and Coniferous Forest classes, a single classified image was produced consisting of both, so that combined they represent all the forest areas in the region in order to facilitate visual analysis (See Figure 12). The classification of the Deep Water class is shown in Figure 13. Figure 14(a) shows the classification results for only the Road Network class; Figures 14(b) and 14(c) are examples of this class taken from the final classification shown in Figure 10, and classification examples of the Shallow Water class, also taken from the final classified image, are presented in Figure 15.

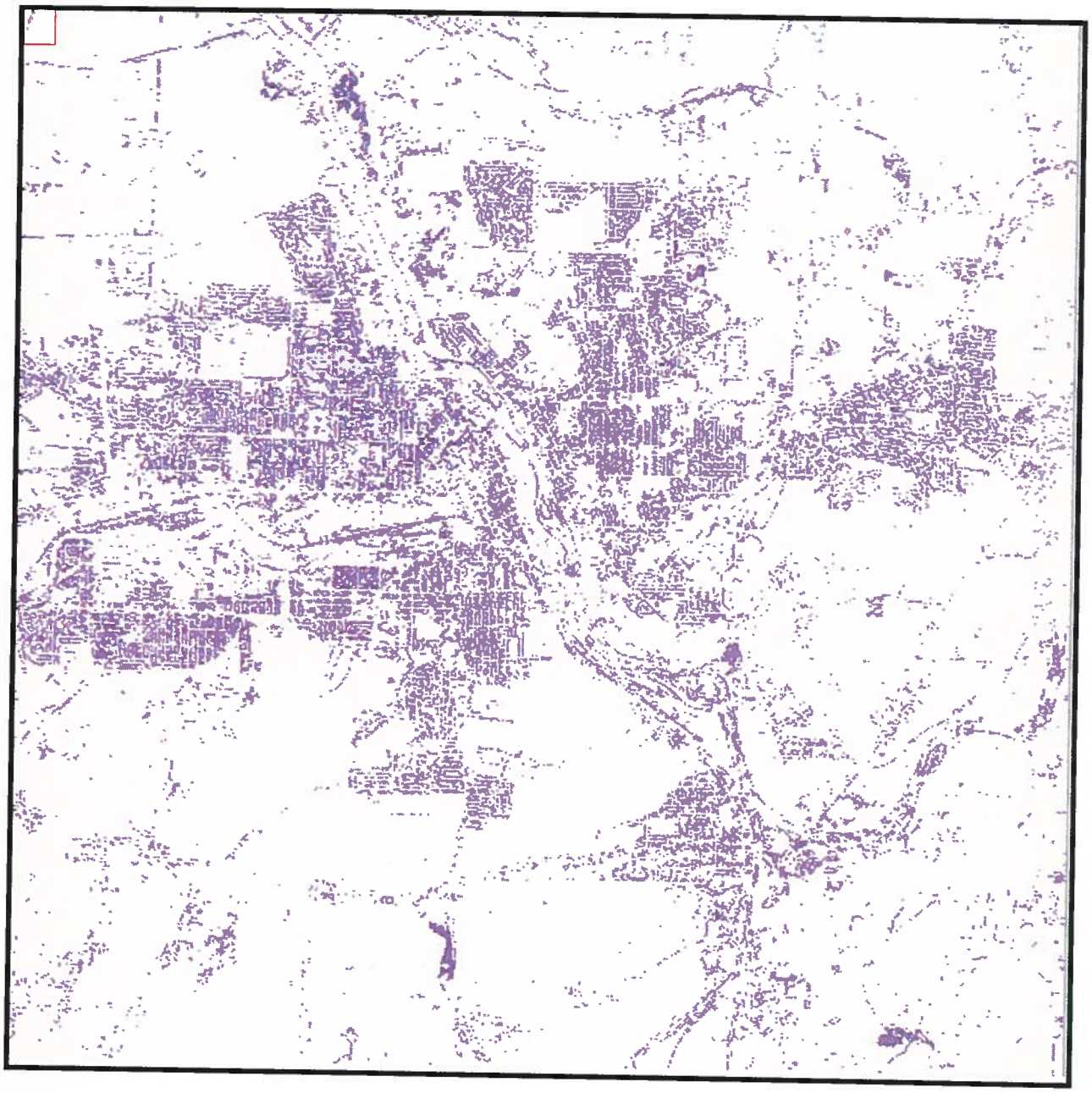

Figure 11: Classified Image of Residential Class

Figure 12: Classified Image of Coniferous and Deciduous Forest Classes

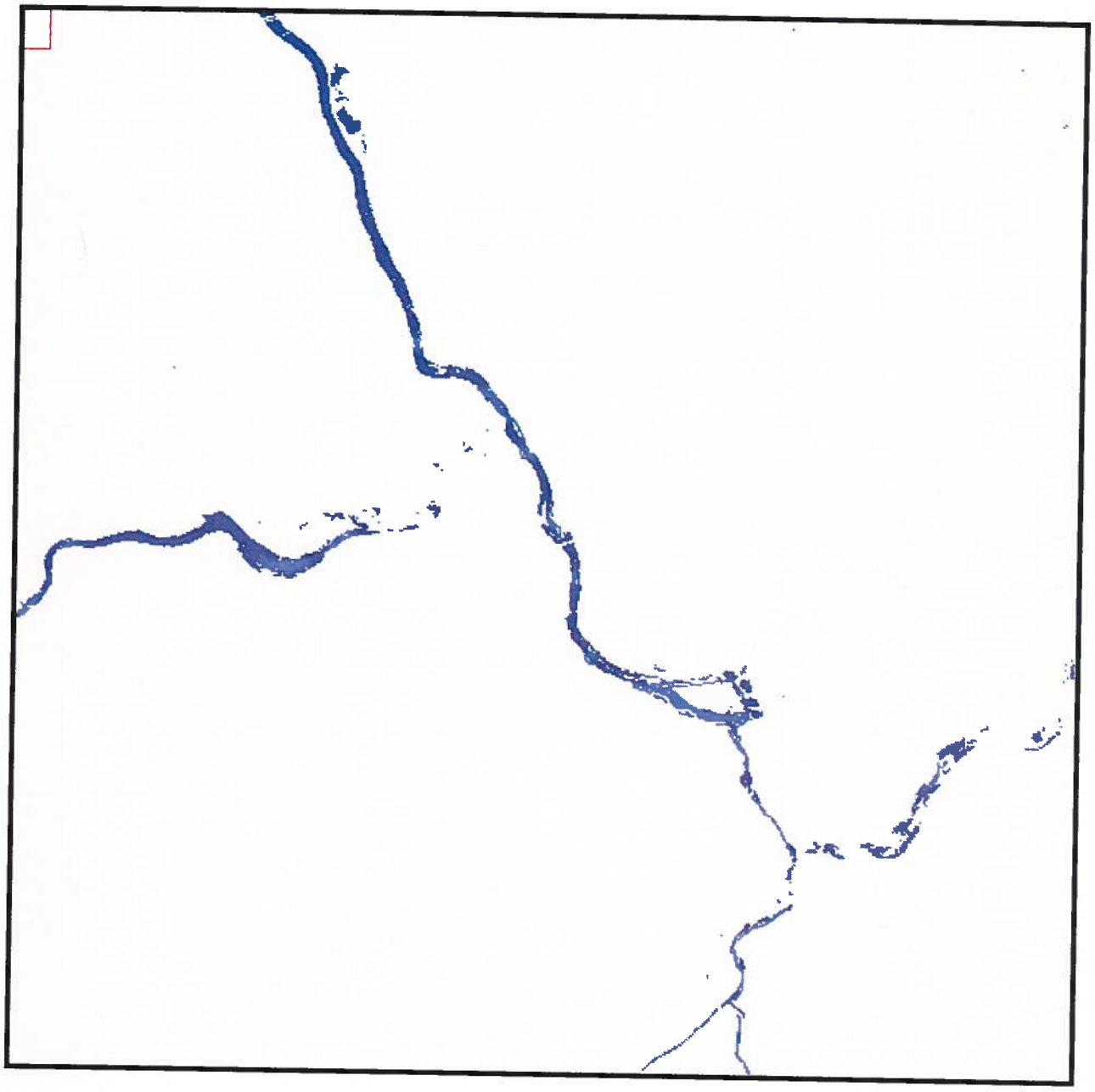

Figure 13: Classified Image of Deep Water Class

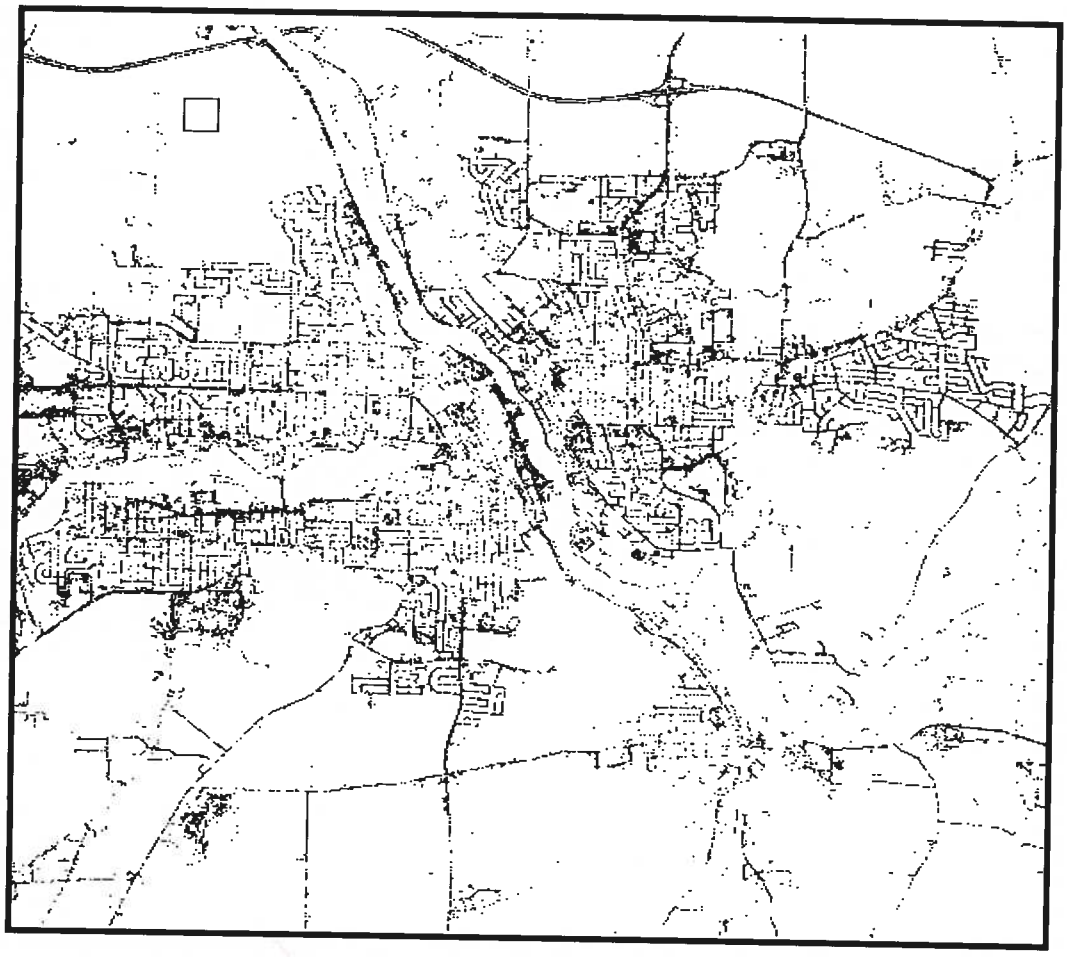

Figure 14(a): Classified Image of Road Network Class

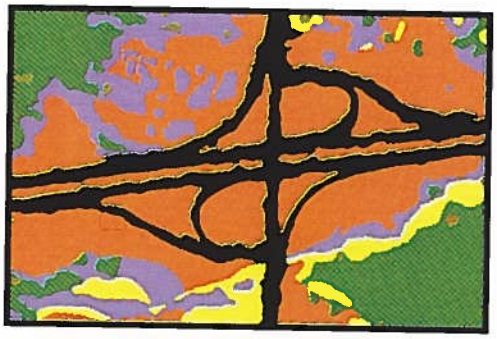

Figure 14(b): Intersection of Highways 10 and 216

Figure 14(c): Jacques-Cartier Bridge

Figure 14: Classified Image and Examples of Road Network Class

Figure 15(a): Section of Magog River adjacent to the beach in Blanchard Park

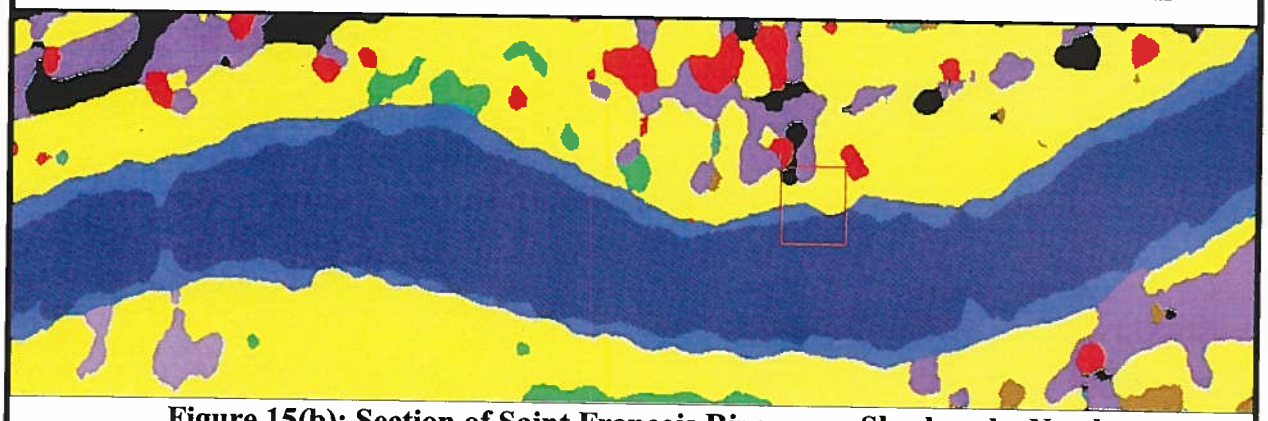

Figure 15(b): Section of Saint François River near Sherbrooke North

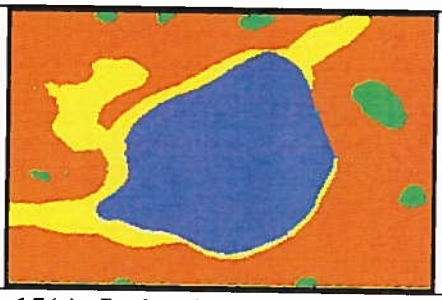

Figure 15(c): Irrigation pond on agricultural plot near Bishop's University in Lennoxville

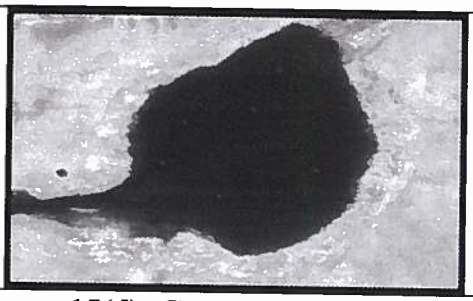

Figure 15(d): Corresponding section of Figure 15(c) from Panchromatic Image

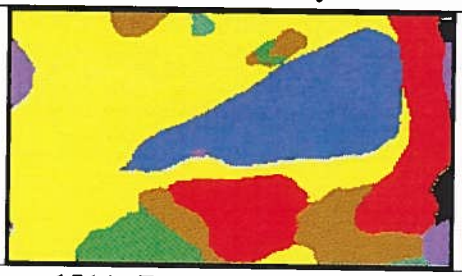

Figure 15(e): Reserved water in a gravel production company at the corner of Bel-Horizon and Dunant streets

Figure 15(f): Corresponding section of Figure 15(e) from Panchromatic Image

Figure 15: Examples of Shallow Water Class from Classified Image

7.4 Discussion

This study has produced results that show classifications based only on textural information provide lower accuracies than classifications performed with purely spectral data. The combination of both types of data for classification, however, produces the highest classification accuracies. Since the classification of the combination dataset in this study provided higher accuracies even on the level of each individual class, this can be attributed to the high spatial resolution of the IKONOS images, which allow for considerable texture discrimination.

These findings are supportive of the hypothesis formulated earlier in this study, that both texture channels and high spatial resolution imagery can provide improved spectral classification accuracies, which result in more detailed urban data. The results are also consistent with various other research studies based on the contribution of texture to spectral classifications, such as that conducted by Moskal and Franklin (2001) who found that classification accuracies of forests based on only texture data were much lower than accuracies for spectral bands of their high-resolution CASI images. They also reported high classification accuracies with the combined data.

From their study using SPOT images, Shaban and Dikshit (2001) also concluded that purely texture features are not effective in classifications of the urban environment. One fact they discovered, however, is that with the addition of textural information, spectral classification accuracies of spectrally homogeneous and distinct classes such as water reduced substantially. The results of the present study are slightly inconsistent on this point, as they display an increase in accuracy for all classes with the combination dataset, although the Deep Water class did produced the lowest increase at only 3.4 %. This difference may be attributed to the higher spatial resolution of the IKONOS images.

Kiema (2002) performed a study on SPOT and Landsat TM images in which the results presented the Homogeneity feature as the most effective co-occurrence matrix texture measure. The texture analysis results of the present study agree with this since it was found that Mean, Homogeneity and Dissimilarity are the best texture features for urban discrimination. However, these results contradict the report by Kiema that a 3x3 pixel window (30x30 m) is the most

suited for urban texture studies, because the most appropriate window size was found to be 11x11 pixels (11x11 m), which is consistent with the work of Moskal and Franklin (2001) who used similar windows (11x11, 17x17, 21x21) to capture the textural characteristics of forest stands. This variation in results may be caused by the higher spatial resolution of the IKONOS imagery.

Overall, the results of this research work support previous studies in respect to the improvement of spectral classifications through the addition of textural data. They differ, though, in areas that are directly related to the texture analysis stage, and mainly from previous research conducted with imagery of a lower spatial resolution. As such, the use of GLCM texture analysis on high spatial resolution IKONOS imagery, combined with the MLC approach, for the improvement of spectral classifications of urban land cover and land use classes provides some interesting results.

Although the results produced in the frame of this work are generally quite high, there are some problem areas. The classification accuracies for two classes, Coniferous Forest and Shrubs, were persistently lower for all datasets. This can be an indication of poor textural representation related to the large size of the 11x11 pixel window. The textural characteristics of certain ground features may require smaller windows. The use of multiple window sizes was not considered due to the heavy computations required for applications on the whole image. Thus, the fact that only one window size was used constitutes one of the limitations of the textural analysis phase of this study. Other limitations of this phase, which may have affected this study, include the use of only one distance, as well as only one direction, between pixels, which were selected either by default of the image processing software employed, or based on their simplicity and popularity. These variables need to be further examined and perhaps can be tested on smaller samples of high-resolution imagery in order to cut down on computational costs.

Future studies within the GLCM texture analysis approach can, therefore, focus on the use of different pixel distances and directions, as well as various window sizes in order to examine their relationship to different types of urban land cover and land use classes for the determination of their contribution to urban texture discrimination of high spatial resolution imagery.

Another study also within the scope of texture analysis that may prove to be very interesting is the separate assessment of the most useful texture features to determine their role in the classification, which might provide some insight into which ground classes they complement the most.

As for the classification phase of the present study, it was found that the problem classes also presented difficulties in spectral discrimination. This can be directly related to the selection of samples for the training and verification sites. Subsequent studies should therefore consider the application of an unsupervised classification technique to first determine the spectral classes that exist in the image, followed by the supervised classification.

7.5 Conclusions

The application of GLCM texture analysis and multispectral MLC techniques for the classification of combined spatial and spectral data for the urban land use and land cover classification of high spatial resolution IKONOS imagery produced very promising results. Some problem areas were encountered, however, related to the limitations of this study.

The texture analysis applied in this study was not comprehensive as it relied on the use of only one window size, which did not permit good textural discrimination of certain ground cover classes, and the use of only one direction and distance between pixels, the effects of which have not been determined. These aspects need to be further studied, based on smaller samples to avoid large computational costs, in order to optimize their application to high spatial resolution imagery.

Another future study based on texture analysis that may be conducted consists of the individual assessment of suitable texture features to determine their relationship to particular ground cover classes, and their impact on urban classifications.

In the spectral classification part of the study, the range of spectral classes contained in the site was not adequately represented. In order to overcome this problem, an unsupervised classification can be performed to detect the existing spectral classes. Then using this information, samples can be selected for the generation of better training and verification sites.

References

Agbu, P.A. and Nizeyimana, E. (1991) Comparisons between spectral mapping units derived from SPOT image texture and field soil map units. Photogrammetric Engineering and Remote Sensing, vol. 57, no. 4, pp. 397-405.

Ahearn, S.C. (1988) Combining Laplacian images of different spatial frequencies (scales): implications for remote sensing analysis. IEEE Transactions on Geoscience and Remote Sensing, vol. 26, pp. 826-831.

Anger, C.D. (1999) Airborne hyperspectral remote sensing in the future? Proceedings of the Fourth International Symposium on Airborne Remote Sensing and 21st Canadian Symposium on Remote Sensing (Ottawa: Canadian Aeronautics and Space institute), pp. 1-15.

Anys, H. (1995) Reconnaissance des cultures à l'aide des images radar: approche multi-polarisation et texturale. Thèse de doctorat, Université de Sherbrooke, Sherbrooke, QC, Canada, 241 p.

Avery, T.E. and Berlin, G.L. (1992) Fundamentals of Remote Sensing and Airphoto Interpretation, Macmillan Publishing Co., New York, 472 p.

Balzerek, H. (2001) Applicability of IKONOS- satellite scenes: monitoring, classification and evaluation of urbanisation processes in Africa. www.rzuser.uni-heidelberg.de, Heidelberg.

Barr, S. and Barnsley, M. (1997) A region-based, graph-theoretic data model for the inference of second-order thematic information from remotely sensed images. International Journal of Geographical Information Sciences, vol. 11, no. 6, pp. 555-576.

Beck, J. (1983) Textural segmentation, second-order statistics, and textural elements. Biological Cybernetics, vol. 48, pp. 125-130.

Beck, J., Sutter, A. and Ivry, R. (1987) Spatial Frequency Channels and Perceptual Grouping in Texture Segregation. Computer Vision, Graphics, and Image Processing, vol. 37, pp. 299-325.

Blostein, D. and Ahuja, N. (1989) Shape from Texture: Integrating Texture-Element Extraction and Surface Estimation, IEEE Transactions on Pattern Analysis and Machine Intelligence, vol. 11, no.12, pp. 1233-1251.

Bruniquel-Pinel, V. and Gastellu-Etchegorry, J.P. (1998) Sensitivity of Texture of High Resolution Images of Forests to Biophysical and Acquisition Parameters. Remote Sensing of the Environment, vol. 65, pp. 61-85.

Campbell, J.B. (1987) Introduction to Remote Sensing. Guilford Press, Cambridge, Massachusetts.

Caylor, K.K., Le, L. and Shugart, H.H. (1999) Structural dynamics in southern African savannas: detecting change through declassified satellite photography. Ecological Society of America Conference, Spokane, Washington, USA.

Chellappa, R. and Kashyap, R.L. (1985) Texture Synthesis using 2-D Noncausal Autoregressive Models. IEEE Transactions on Acoustics, Speech, and Signal Processing, vol. 33, no. 1, pp. 194-203.

Chen, Y. and Dougherty, E.R. (1994) Greyscale morphological granulometric texture classification. Optical Engineering, vol. 33, pp. 2713-2722.

Conners, R.W, Trivedi, M.M. and Harlow, C.A. (1984) Segmentation of a high-resolution urban scene using texture operators. Computer Vision, Graphics, and Image Processing, vol. 25, pp. 273-310.

Coggins, J. M. (1982) A Framework for Texture Analysis Based on Spatial Filtering. PhD. Thesis, Computer Science Department, Michigan State University, East Lansing, Michigan, USA.

Congalton, R. G. (1991) A review of assessing the accuracy of classifications of remotely sensed images. Remote Sensing of the Environment, vol. 37, pp. 35-46.

Coulombe, A., Charbonneau, L., Brochu, R. et Morin, D. (1991) L'apport de l'analyse texturale dans la définition de l'utilisation du sol en milieu urbain. Journal canadien de télédétection, vol. 17, no. 1, pp. 46-55.

Cushnie, J.L. (1987) The interactive effects of spatial resolution and degree of internal variability within land cover type on classification accuracies. International Journal of Remote Sensing, vol. 8, no. 1, pp. 15-22.

D'Astous, F. and Jernigan, M.E. (1984) Texture Discrimination Based on Detailed Measures of the Power Spectrum. Proceedings of IEEE Computer Society Conference on Pattern Recognition and Image Processing, pp. 83-86.

Dimyati, M., Mizuno, K., Kobayashi, S. and Kitamura, T. (1996) An analysis of land use/cover change using the combination of MSS Landsat and land use map--a case study in Yogyakarta, Indonesia. International Journal of Remote Sensing, vol. 17, no. 5, pp. 931-944.

Franklin, S.E., Hall, R.J., Moskal, L.M., Maudie, A.J. and Lavigne, M.B. (2000) Incorporating texture into classification of forest species composition from airborne multispectral images. International Journal of Remote Sensing, vol. 21, no. 1, pp. 61-79.

Franklin, S.E., Wulder, M.A. and Gerylo, G.R. (2001) Texture Analysis of IKONOS panchromatic data for Douglas-fir forest age class separability in British Columbia. International Journal of Remote Sensing, vol. 22, no. 13, pp. 2627-2632.

Franklin, S.E. and McDermid, G.J. (1993) Empirical relations between digital SPOT HRV and CASI spectral response and lodgepole pine forest stand parameters. International Journal of Remote Sensing, vol. 14, no. 12, pp. 2331-2348

Franklin, S.E. and Peddle, D.R. (1989) Spectral texture for improved class discrimination in complex terrain. International Journal of Remote Sensing, vol. 10, no. 8, pp. 1437-1443.

Franklin, S.E. and Peddle, D.R. (1990) Classification of SPOT HRV imagery and texture features. International Journal of Remote Sensing, vol. 11, no. 3, pp. 551-556.

Fung, T. and Ledrew, E. (1988) The determination of optimal threshold levels for change detection using various accuracy indices. Photogrammetric Engineering and Remote Sensing, vol. 54, no. 10, pp. 1449-1454.

Gong, P. (1990) Improving accuracies in land use classification with high spatial resolution satellite: a contextual classification approach. PhD Thesis, University of Waterloo, Waterloo, ON, Canada, 181 p.

Gong, P., Marceau, D. and Howarth, P. J. (1992) A comparison of spatial feature extraction algorithms for land use classification with SPOT HRV data. Remote Sensing of the Environment, vol. 40, pp. 137-151.

Goresnic, C. and Rotman, S.R. (1992) Texture classification using the cortex transform. Computer Vision, Graphics, and Image Processing: Graphical Models and Image Processing, vol. 54, pp. 329-339.

Green, K. (2000) Selecting and interpreting high-resolution images. Journal of Forestry, vol. 98, pp. 37-39

Haala, N. and Brenner, C. (1999) Extraction of building and trees in urban environments. Photogrammetric Engineering and Remote Sensing, vol. 54, pp. 130-137.

Haralick, R.M., Shanmugan, K. and Dinstein, I. (1973) Textural features for image classification. IEEE, Transactions on Systems, Man, and Cybernetics, vol. 8, pp. 610-621.

Haralick, R.M. (1979) Statistical and structural approaches to texture. Proceedings of the IEEE, vol. 67, no. 5, pp. 786-804.

Haralick, R.M. (1986) Statistical image texture analysis. In Young, T.Y. and Fu, K.S. (eds.), Handbook of Pattern Recognition and Image Processing, Academic Press, New York, pp. 247-280.

Haralick, R. and Shapiro, L. (1992) Computer and Robot Vision, Volume 1. Addison-Wesley, Massachusetts.

Hay, G.J. and Niemann, K.O. (1994) Visualizing 3D texture: a three dimensional structural approach to model forest texture. Canadian Journal of Remote Sensing, vol. 20, pp. 90-101.

Hay, G.J., Niemann, K.O. and McLean, G.F. (1996) An object-specific image-texture analysis of high-resolution forest imagery. Remote Sensing of the Environment, vol. 55, p. 108-122.

Hawkins, J. K. (1969) Textural Properties for Pattern Recognition. In Lipkin, B. and Rosenfeld, A. (eds.), Picture Processing and Psychopictorics, Academic Press, New York.

He, D.-C., Wang, L. and Guibert, J. (1987) Texture Feature Extraction. Pattern Recognition Letters, vol. 6, pp. 269-273.

He, D.-C. and Wang, L. (1991) Texture features based on texture spectrum. Pattern Recognition, vol. 24, no. 5, pp. 391-399.

Holecz, F., Meier, E. and Nüesch, D. (1993) Postprocessing of relief induced radiometric distorted spaceborne SAR imagery. In Schreier, G. (ed.), SAR Geocoding: Data and Systems, Wichmann, Karlsruhe, pp. 299-352.

Hudak, A.T. and Wessman, C.A. (1998) Textural Analysis of Historical Aerial Photography to Characterize Woody Plant Encroachment in South African Savanna. Remote Sensing of the Environment, vol. 66, pp. 317-330.

Irons, J.R., Markham, B.L., Nelson, R.F., Toll, D.L., Williams, D.L., Latty, R.S. and Stauffer, M.L. (1985) The effects of spatial resolution on the classification of Thematic Mapper data. International Journal of Remote Sensing, vol. 6, no. 8, pp. 1385-1403.

Jakubauskas, M.E. (1997) Effects of forest succession on texture in Landsat TM imagery. Canadian Journal of Remote Sensing, vol. 23, no. 3, pp. 257-163.

Jensen, J.R. (1996) Introductory Digital Image Processing. 2nd edition, Prentice-Hall, New Jersey, 318 p.

Jensen, J.R. (2000) Remote Sensing of the Environment: An Earth Resource Perspective. Prentice-Hall, New Jersey, 336 p.

Julesz, B. (1962) Visual Pattern Discrimination. IRE Transactions on Information Theory, vol. 8, pp. 84-92.

Julesz, B. (1975) Experiments in the visual perception of texture. Scientific American, vol. 232, pp. 34-43.

Julesz, B. (1981a) Textons, the elements of texture perception, and their interactions. Nature, vol. 290, pp. 91-97.

Julesz, B. (1981b) A Theory of Preattentive Texture Discrimination Based on First-order Statistics of Textons. Biological Cybernetics, vol. 41, pp. 131-138.

Julesz, B., Gilbert, E.N., Shepp, L.A. and Frisch, H.L. (1973) Inability of humans to discriminate between visual textures that agree in second-order statistics – revisited. Perception, vol. 2, pp. 391-405

Julesz, B. and Bergen, R. (1983) Textons, the fundamental elements in preattentive vision and perception of texture. The Bell System Technical Journal, vol. 62, no.6, pp. 1619-1645.

Kaiser, H. (1995) A Quantification of Texture on Aerial Photographs. Boston University, Research Lab, Technical Note 121, AD69484.

Karathanassi, V., Iossifidis, C.H. and Rokos, D. (2000) A texture-based classification method for classifying built areas according to their density. International Journal of Remote Sensing, vol. 21, no. 9, pp. 1807-1823.

Kershaw, C.D. and Fuller, R.M. (1992) Statistical problems in the discrimination of land cover from satellite images: a case study in lowland Britain. International Journal of Remote Sensing, vol. 13, pp. 3085-3104.

Kiema, J.B.K. (2002) Texture analysis and data fusion in the extraction of topographic objects from satellite imagery. International Journal of Remote Sensing, vol. 23, no. 4, pp. 767-776.

Kilpelä, E. and Heikilä, J. (1990) Comparison of Some Texture Classifiers. Proceedings of the Symposium on Global and Environmental Monitoring Techniques and Impact, Victoria, British Columbia, Canada, September 17-21, vol. 28, part 7.2, pp. 333-339.

King, D. (1995) Airborne Multispectral Digital Camera and Video Sensors: A Critical Review of System Designs and Applications. Canadian Journal of Remote Sensing, vol. 21, no. 3, pp. 245-273.

Kourgli, A. and Belhadj-Aissa, A. (2000) Textural Classification using Textural Signatures. In Casanova, J.L. (ed.), Proceedings of the European Association of Remote Sensing Laboratories (EARSeL) Symposium: Remote Sensing in the 21st Century, Economic and Environmental Applications, A.A. Balkema, Rotterdam, pp. 557-561.

Kurosu, T., Yokoyama, S. and Fujita, M. (2001) Land use classification with textural analysis and the aggregation technique using multi-temporal JERS-1 L-band SAR images. International Journal of Remote Sensing, vol. 22, no. 4, pp. 595-613.

Kushwaha, S.P.S., Kuntz, S. and Oesten, G. (1994) Applications of image texture in forest classification. International Journal of Remote Sensing, vol. 15, no. 11, pp. 2273-2284.

Laws, K.I. (1980) Textured Image Segmentation. PhD. Thesis, University of Southern California, CA, USA.

Laur, H. (1989) Analyse d'images radar en télédétection: discriminateurs radiométriques et texturaux. Thèses de doctorat, Université Paul Sabatier, no. 403, Toulouse, 244 p.

Leckie, D.G., Beaubien, J., Gibson, J.R., O'Neil, N.T., Piekutowski, T. and Joyce, S.P. (1995) Data processing and analysis for MIFUCAM: a trial of MEIS imagery for forest inventory mapping. Canadian Journal of Remote Sensing, vol. 21, no. 3, pp. 337-356.

Li, W., Bénié, G.B., He, D.-C., Wang, S., Ziou, D. and Gwyn, Q.H.J. (1998) Classification of SAR images using morphological texture features. International Journal of Remote Sensing, vol. 19, no. 17, pp. 3399-3410.

Lo, C.P. and Shipman, R.L. (1990) A GIS approach to land-use change dynamics detection. Photogrammetric Engineering and Remote Sensing, vol. 56, no. 11, pp. 1483-1491.

Matsuyama, T., Miura, S.I. and Nagao, M. (1980) Structural Analysis of Natural Textures by Fourier Transformation. Computer Vision Graphics Image Processing, vol. 12, pp. 286-308.

Marceau, D.J. (1988) Apport de l'analyse texturale à la classification automatisée d'un environnement côtier de région tempérée à La Baie des Chaleurs, Québec, d'après des données SPOT. Mémoire de maîtrise, Département de géographie et télédétection, Université de Sherbrooke, Sherbrooke, QC, Canada, 88 p.

Marceau, D.J., Howarth, P.J., Dubois, J.M. and Gratton, D.J. (1990) Evaluation of the grey level co-occurrence matrix for land cover classification using SPOT imagery. I.E.E.E. Transactions on Geoscience and Remote Sensing, vol. 28, no. 4, pp. 513-519.

Miranda, F.P., MacDonald, J.A. and Carr, J.R. (1996) Analysis of JERS-1 (Fuyo-1) SAR data for vegetation discrimination in northwestern Brazil using the semivariogram textural classifier (STC). International Journal of Remote Sensing, vol. 17, pp. 3523-3529.

Marr, D. (1976) Early Processing of Visual Information. Philosophical Transactions of the Royal Society of London, Series B, vol. 275, pp. 483-524.

Marr, D. (1982) Vision, a computational investigation into the human representation and processing of visual information. W.H. Freeman, New York.

Mather, P.M., Tso, B. and Koch, M. (1998) An evaluation of the Landsat TM spectral data and SAR-derived textural information for lithological discrimination in the Red Sea Hills, Sudan. International Journal of Remote Sensing, vol. 19, no. 4, pp. 587-604.

Møller-Jensen, L. (1990) Knowledge-based classification of an urban area using texture and context information in Landsat-TM imagery. Photogrammetric Engineering and Remote Sensing, vol. 56, no. 6, pp. 899-904.

Moskal, L.M. and Franklin, S.E. (2001) Classifying multilayer forest structure and composition using high resolution Compact Airborne Spectrographic Imager CASI image texture, Research Report, Department of Geography, University of Kansas, USA.

Nellis, M.D., Lulla, K. and Jenson, J. (1990) Interfacing geographic information systems and remote sensing for rural land-use analysis. Photogrammetric Engineering and Remote Sensing, vol. 56, no. 3, pp. 329-331.

Ndi Nyoungui, A., Tonye, E. and Akono, A. (2002) Evaluation of speckle filtering and texture analysis methods for land cover classification from SAR images. International Journal of Remote Sensing, vol. 23, no. 9, pp. 1895-1925.

Ober, G., Tomasoni, R. and Cella, F. (1997) Urban Texture Analysis. International Symposium on Optical Science Engineering and Instrumentation, July-August 1997, San Diego, CA, USA.

Pathan, S.K., Sastry, S.V.C. and Dhinea, P.S. (1993) Urban growth trend analysis using GIS techniques-a study of the Bombay metropolitan region. International Journal of Remote Sensing, vol. 14, no.17, pp. 3169-3176.

Pesaresi, M. and Bianchin, A. (2001) Recognizing settlement structure using mathematical morphology and image texture. In Donnay, J.P, Barnsley, M.J. and Longley, P.A. (eds.), Remote Sensing and Urban Analysis, London, pp. 56-67.

Pickett, R.M. (1970) Visual analysis of texture in the detection and recognition of objects. Picture Processing and Psychopictorics (Lipkin, B.C. and Rosenfeld, A., eds.), Academic Press, New York, pp. 298-308.

Pratt, W.K., Faugeras, O.D. and Gagalowicz, A. (1973) Visual Discrimination of stochastic texture fields. IEEE Transactions on Systems, Man and Cybernetics, vol. 8, no. 11, pp. 796-804.

Pultz, T.J. and Brown, R.J. (1987) SAR image classification of agricultural targets using first- and second-order statistics. Canadian Journal of Remote Sensing, vol. 13, no. 2, pp. 85-91.

Richards, W. and Polit, A. (1974) Texture matching, Kybernetic, vol. 16, pp. 155-162.

Richards, J.A. and Jia, X. (1999) Remote sensing digital image analysis: an introduction. 3rd edition, New York: Springer-Verlag, 363 p.

Roberts, A. (1995) Integrated MSV airborne remote sensing. Canadian Journal of Remote Sensing, 21, pp. 214-224.

Ryherd, S. and Woodcock, C. (1996) Combining spectral and texture data in the segmentation of remotely sensed images. PE & RS 62(2): pp. 181-194.

Sali, E. and Wolfson, H. (1992) Texture Classification in Aerial Photographs and Satellite Data. International Journal of Remote Sensing, vol. 13, no. 18, pp. 3395-3408.

Shaban, M.A. and Dikshit, O. (2001) Improvement of classification in urban areas by the use of textural features: the case study of Lucknow city, Uttar Pradesh. International Journal of Remote Sensing, Vol. 22, No. 4, pp. 565-593.

Schatz, B.R. (1977) Computation of Immediate Texture Discrimination. Proceedings of the 5th International Joint Conference on Artificial Intelligence, pp. 708.

Schowengerdt, R.A. (1997) Remote Sensing: Models and Methods for Image Processing. 2nd edition, San Diego, Academic Press.

Sklansky, J. (1978) Image Segmentation and Feature Extraction, IEEE Transactions on Systems, Man, and Cybernetics, SMC-8, pp. 237-247.

Slimani, M. (1986) Analyse de texture en télédétection: application a la segmentation d'images satellites à haute résolution type SPOT. PhD Thesis, Université de Rennes, 82 p.

Smith, G.M. and Fuller, R.M. (2001) An integrated approach to land cover classification: an example in the Island of Jersey. International Journal of Remote Sensing, Vol. 22, No. 16, pp. 3123-3142.

Stoney, W. E. and Hughes, J. R. (1998) A New Space Race Is On! GIS World (March 1998).

Terzopoulos, D. (1980) Applying Co-occurrence Matrices to Texture classification, M.Sc. Thesis, Mcgill University, Quebec, Canada, 163 p.

Tamura, H., Mori, S. and Yamawaki, T. (1978) Textural Features Corresponding to Visual Perception," IEEE Transactions on Systems, Man, and Cybernetics, vol. 8, pp. 460-473.

Tomita, F. and Tsuji, S. (1990) Computer Analysis of Visual Textures. Kluwer Academic Publishers, London, 173 p.

Tomita, F., Shirai, Y. and Tsuji, S. (1982) Description of textures by a structural analysis. IEEE Transactions, PAMI-4, pp. 183-191.

Townshend, J.R.G. (1981) The spatial resolving power of earth resources satellites. Progress in Physical Geography, 5: pp.32-55.

Tso, B. (1997) The investigation of alternative strategies for incorporating spectral, textural and contextual information in remote sensing image classification. PhD Thesis, Department of Geography, University of Nottingham, UK.

Tuceryan, M. and Jain, A.K. (1998) Texture Analysis, The Handbook of Pattern Recognition and Computer Vision (2nd Edition), P. S. P. Wang (eds.), pp. 207-248, World Scientific Publishing Co.

Turner, B.L. and Meyer, W.B. (1994) Changes in the land use land cover: A global perspective. Cambridge University Press, Great Britain, pp. 1-9.

Unser, M. (1984) Description statistique de textures: application à l'inspection automatique. PhD. Thèse, École Polytechnique Fédéral de Lausanne, 201 p.

Unser, M. (1986) Sum and difference histograms for texture classification. IEEE Transactions on Pattern Analysis and Machine Intelligence, vol. 8, no. 1, pp. 118-125.

Voorhees, H. and Poggio, T. (1987) Detecting textons and texture boundaries in natural images. Proceedings of the First International Conference on Computer Vision, London, pp. 250-258,

Wang, L. and He, D.-C. (1990) A new statistical approach for texture analysis. Photogrammetric Engineering and Remote Sensing, vol. 55, pp. 61-66

Welch, R. (1982) Spatial resolution requirement for urban studies. International Journal of Remote Sensing, vol.6, p. 139-157.

Weszka, J.S., Dyer, C.R. and Rosenfeld, A. (1976) A comparative study of texture measures for terrain classification, IEEE, Transaction on System, Man and Cybernetics, vol. 6, no. 4, pp. 269-285.

Wilson, B.A. (1996) Estimating Conifer Structure using SAR Texture Analysis. PhD Thesis, University of Calgary, Alberta.

Zhang, Y. (1999) Optimization of building detection in satellite images by combining multispectral classification and texture filtering. ISPRS Journal of Photogrammetry and Remote Sensing, vol. 54, pp. 50-60.

Zucker, S. W. and Kant, K. (1981) Multiple-level Representations for Texture Discrimination, In Proceedings of the IEEE Conference on Pattern Recognition and Image Processing, Dallas, Texas, pp. 609-614.

Zucker, S. W. and Cavanaugh, P. (1985) Subjective figures and texture perception. Technical Report TR-85-R2, Computer Vision and Robotics Laboratory, Department of Electrical Engineering, McGill University, Quebec, Canada.

Appendix A: Satellite and Texture Images

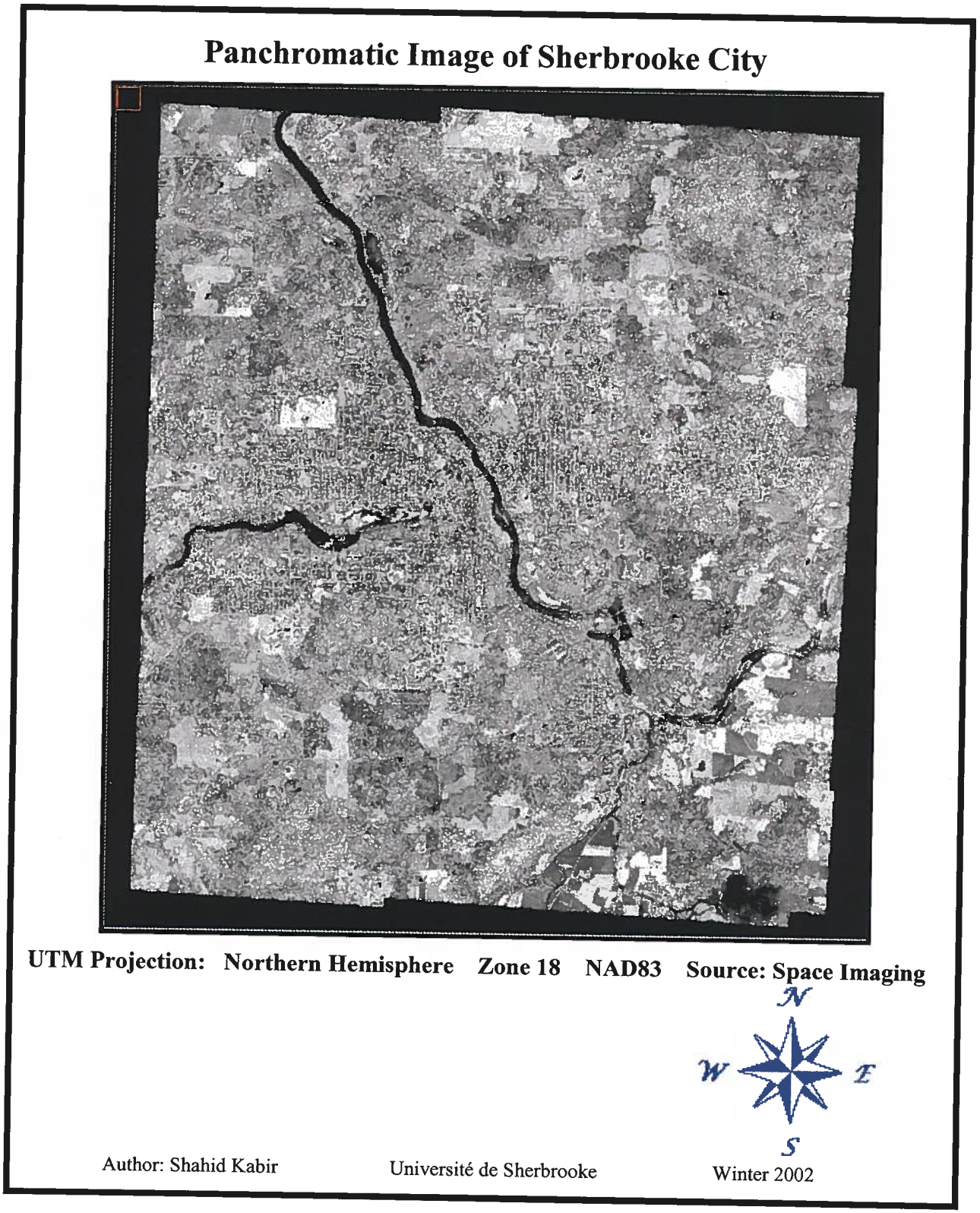

Figure 16: Raw Panchromatic IKONOS Image of Sherbrooke City

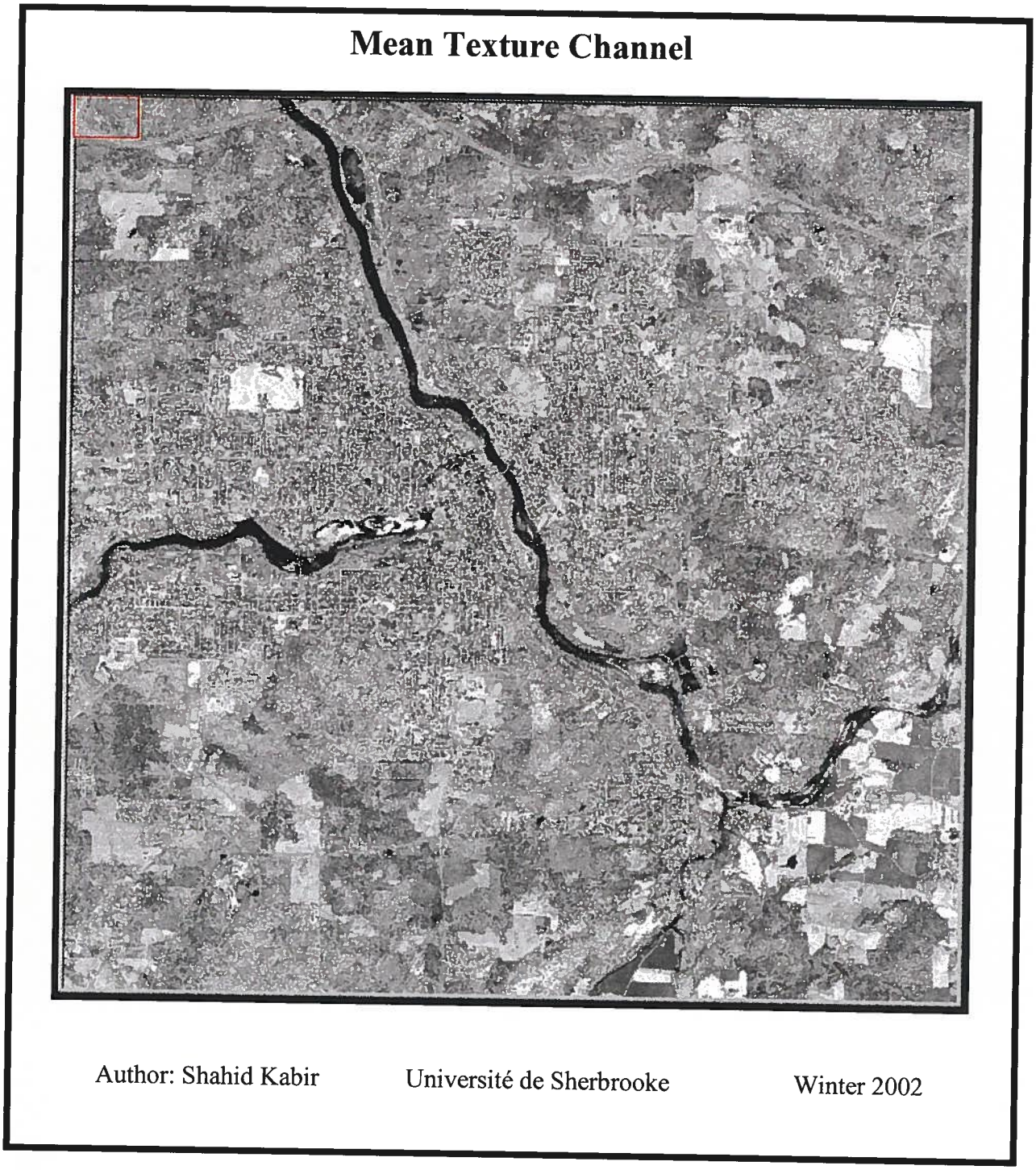

Figure 17: Mean Texture Channel of Sherbrooke Study Region

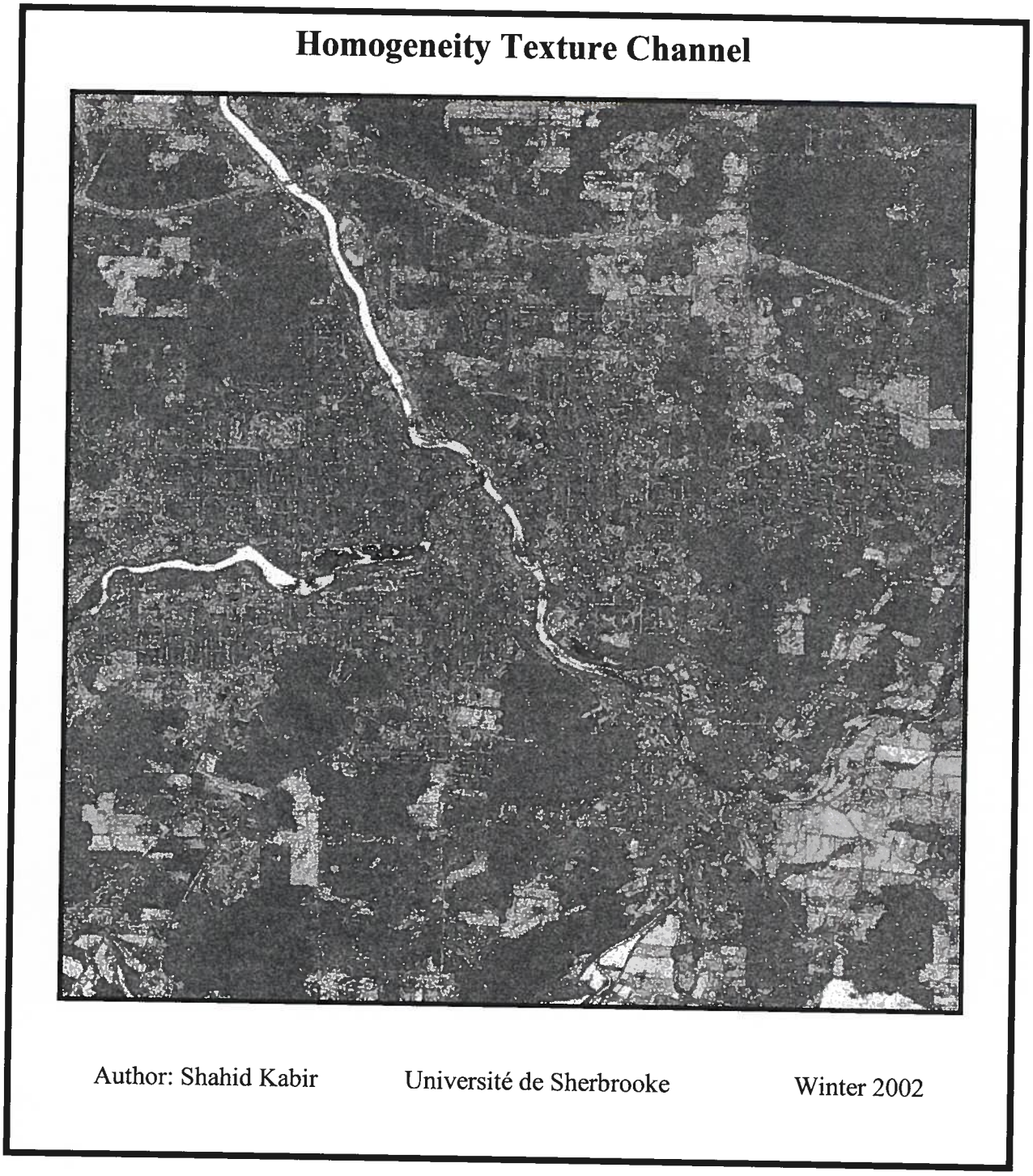

Figure 18: Homogeneity Texture Channel of Sherbrooke Study Region

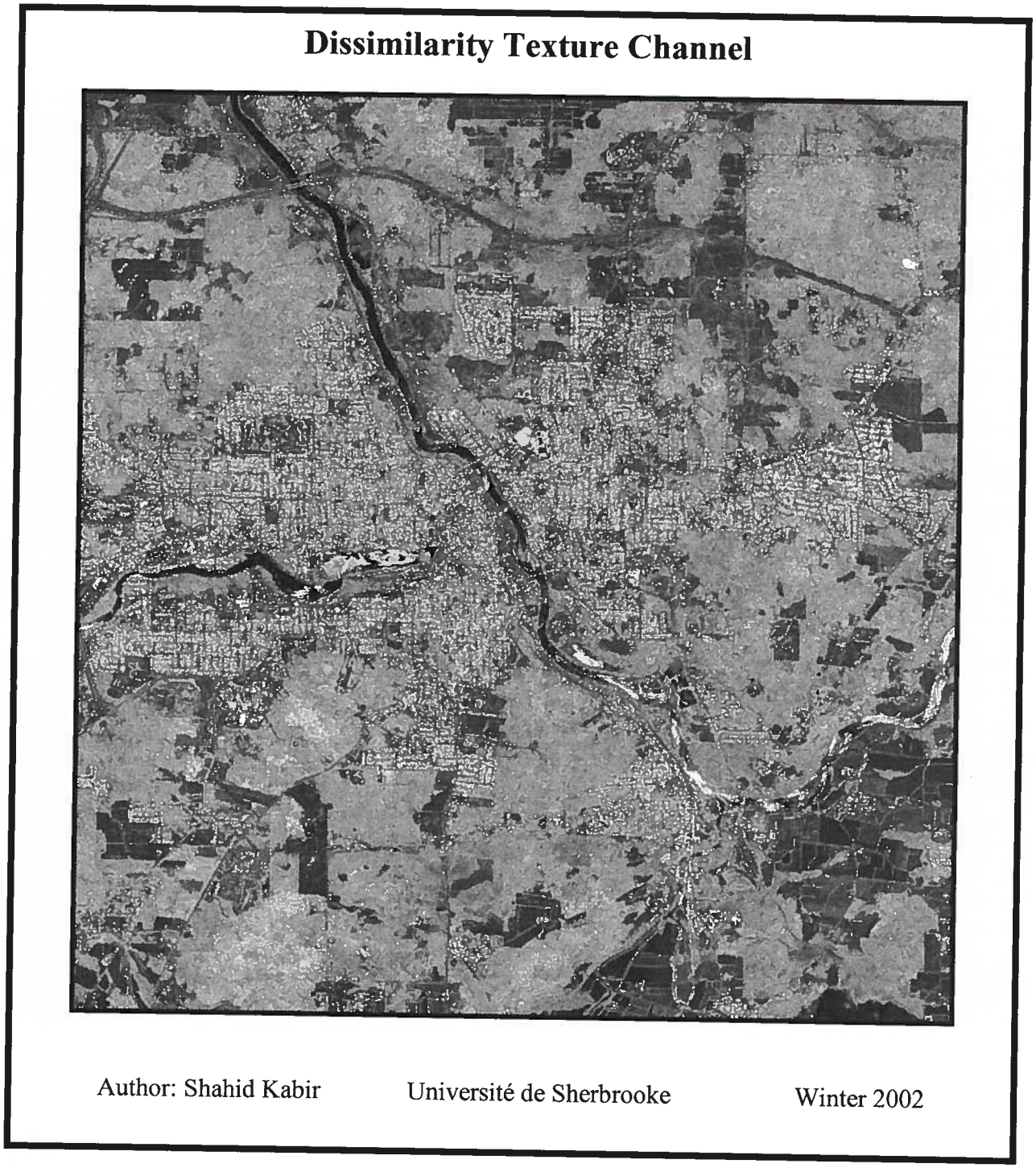

Figure 19: Dissimilarity Texture Channel of Sherbrooke Study Region

Appendix B: Statistics of Results

Filename: Sherbrooke Panchromatic Image

Texture Method: Co-occurrence Matrix

Window Size: 11x11 pixels

Distance: 1 pixel

Direction: 0 degrees

Dims: Full Band (121000000 points)

Channels	Min	Max	Mean	Standard Deviation
Mean	0.000000	2046.975342	378.633742	93.302780
Variance	0.000000	734680.062500	5934.594641	14027.790953
Homogeneity	0.000000	0.975207	0.035399	0.026361
Contrast	0.000000	1016408.062500	4845.880744	11972.567280
Dissimilarity	0.000000	745.380127	42.114551	22.330366
Entropy	0.000000	4.795791	4.774688	0.219402
Second Moment	0.000000	0.904515	0.008423	0.002299
Correlation	-9327.056641	0.092787	-23.814306	82.321651

Table 6: Statistics of Texture Bands

Class Pairs	J-M	Class Pairs	TD
Deciduous Forest & Shrubs	1.49961513	Bare Soil & Parking Lot	1.91528622
Agricultural Land & Road Network	1.50507418	Coniferous Forest & Road Network	1.95922871
Coniferous Forest & Residential Area	1.51039070	Bare Soil & Agricultural Land	1.96127155
Coniferous Forest & Deciduous Forest	1.51131622	Commercial & Deep Water	1.97004509
Commercial & Parking Lot	1.51284186	Grass & Shrubs	1.97124861
Commercial & Residential Area	1.52500401	Bare Soil & Road Network	1.97323637
Coniferous Forest & Shrubs	1.53112276	Shallow Water & Parking Lot	1.97881723
Road Network & Shrubs	1.53280035	Bare Soil & Shallow Water	1.98120044
Agricultural Land & Commercial	1.53623525	Agricultural Land & Coniferous Forest	1.98234294
Shallow Water & Deep Water	1.54722153	Grass & Deciduous Forest	1.98763208
Commercial & Shrubs	1.55821074	Deep Water & Residential Area	1.98827635
Deciduous Forest & Road Network	1.56099882	Bare Soil & Coniferous Forest	1.99483292
Commercial & Road Network	1.56577646	Bare Soil & Deep Water	1.99485691
Commercial & Deciduous Forest	1.57827307	Bare Soil & Deciduous Forest	1.99506599
Commercial & Coniferous Forest	1.57998630	Deep Water & Parking Lot	1.99581734
Bare Soil & Commercial	1.61322964	Bare Soil & Shrubs	1.99610998
Grass & Commercial	1.62224905	Shallow Water & Coniferous Forest	1.99613878
Grass & Agricultural Land	1.63235572	Residential Area & Road Network	1.99644104
Parking Lot & Residential Area	1.63679587	Agricultural Land & Residential Area	1.99729682
Agricultural Land & Shrubs	1.67679256	Grass & Bare Soil	1.99909450
Parking Lot & Shrubs	1.68610948	Grass & Coniferous Forest	1.99988725
Parking Lot & Deciduous Forest	1.72776165	Grass & Residential Area	1.99999149
Coniferous Forest & Parking Lot	1.76505063	Deep Water & Coniferous Forest	1.99999205
Grass & Road Network	1.76936710	Shallow Water &.Deciduous Forest	1.99999453
Parking Lot & Road Network	1.77642367	Deep Water & Deciduous Forest	2.00000000
Bare Soil & Residential Area	1.81522157	Agricultural Land & Shallow Water	2.00000000
Agricultural Land & Deciduous Forest	1.82253444	Shallow Water & Shrubs	2.00000000
Agricultural Land & Parking Lot	1.82948679	Shallow Water & Road Network	2.00000000
Deciduous Forest & Residential Area	1.85226770	Grass & Shallow Water	2.00000000
Residential Area & Shrubs	1.86209483	Deep Water & Road Network	2.00000000
Commercial & Shallow Water	1.86463105	Grass & Deep Water	2.00000000
Shallow Water & Residential Area	1.87153773	Deep Water & Shrubs	2.00000000
Grass & Parking Lot	1.90480444	Agricultural Land & Deep Water	2.00000000

Table 7: Class Pair Separabilities using Jeffries-Matusita (J-M) and Transformed Divergence (TD) Measures